

Chemistry—A European Journal

Supporting Information

Photoswitching Affinity and Mechanism of Multivalent Lectin Ligands

Uwe Osswald, Johannes Boneberg, and Valentin Wittmann*

Author Contributions

U.O. Conceptualization:Equal; Data curation:Equal; Investigation:Lead; Writing – original draft:Lead; Writing – review & editing:Equal

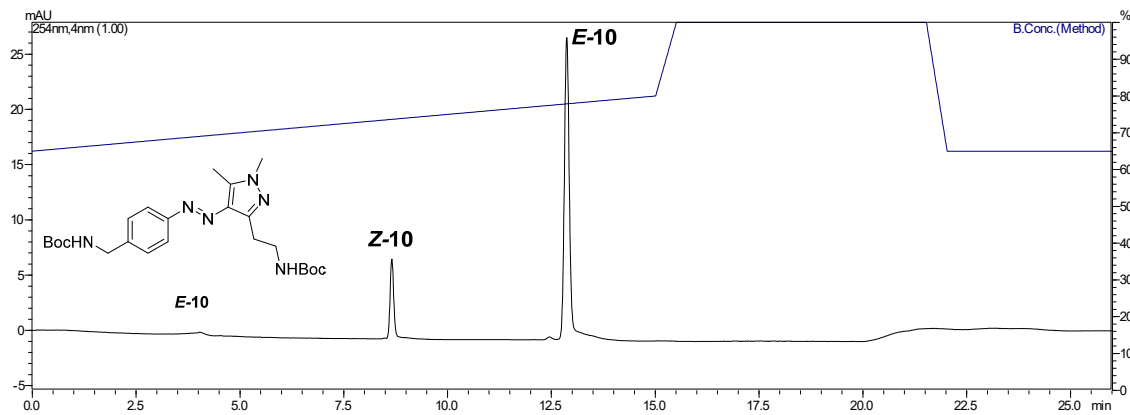
J.B. Conceptualization:Equal; Data curation:Equal; Investigation:Supporting

V.W. Conceptualization:Lead; Data curation:Lead; Supervision:Lead; Writing – review & editing:Lead

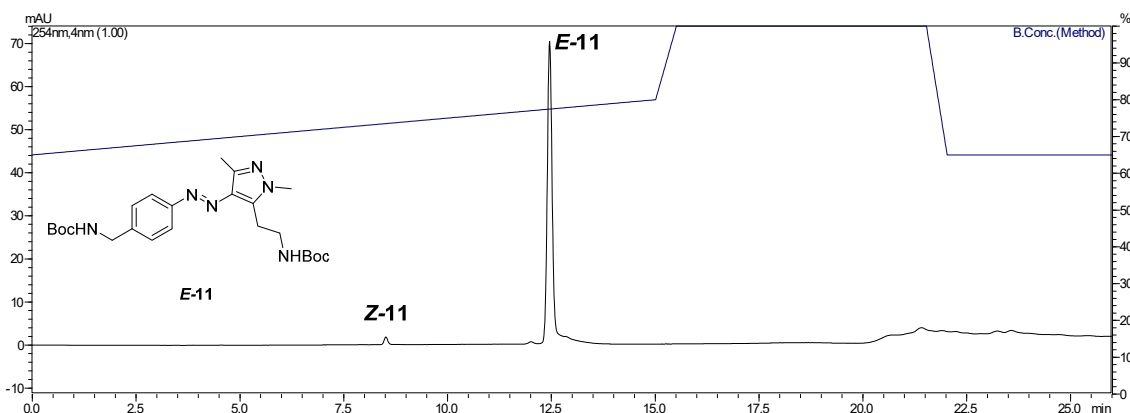
Supporting Information

1. Chromatograms of Photoswitches	S2
2. Determination of Quantum Yields.....	S5
3. Determination of Thermal Half-Life.....	S11
4. ITC Experiments.....	S13
5. DLS Data	S19
6. Possible Structure of WGA in Complex with Z-3.....	S21
7. NMR Spectra.....	S22
8. References.....	S30

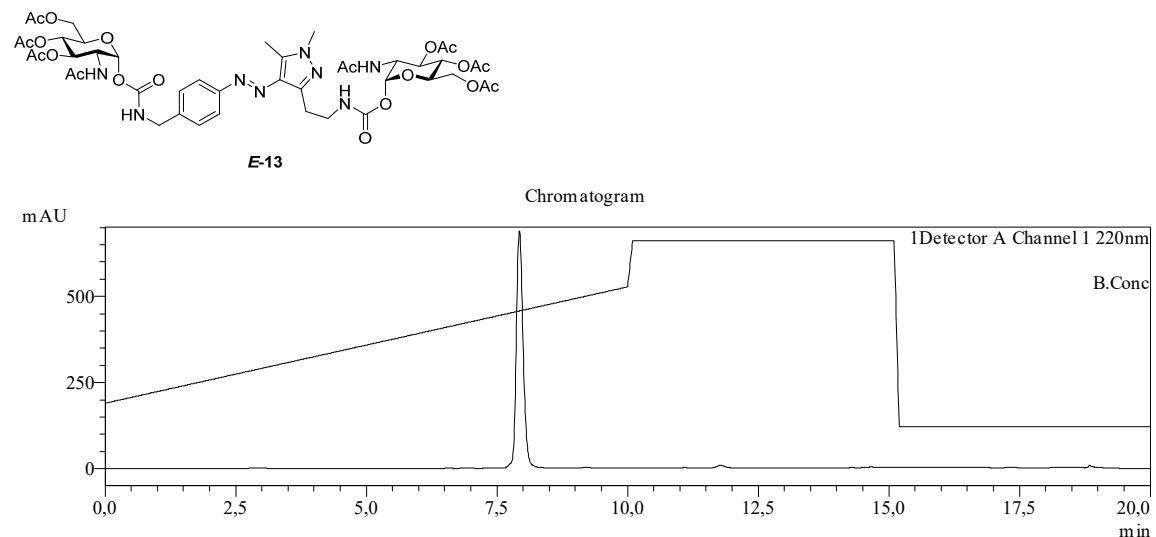
1. Chromatograms of Photoswitches



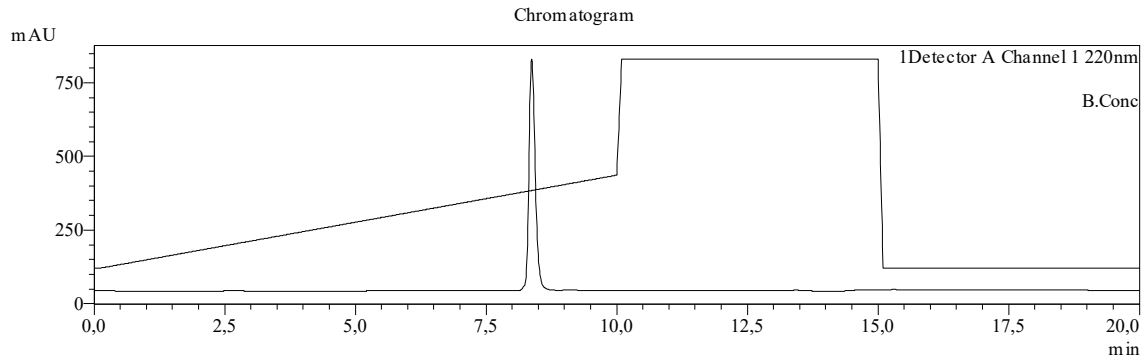
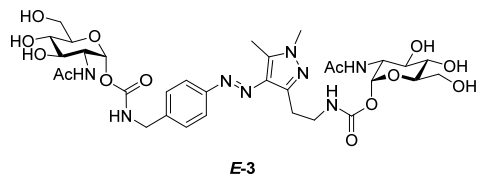
Semi-preparative HPLC profile of **E/Z-10** (65–80% MeCN in 15 min).



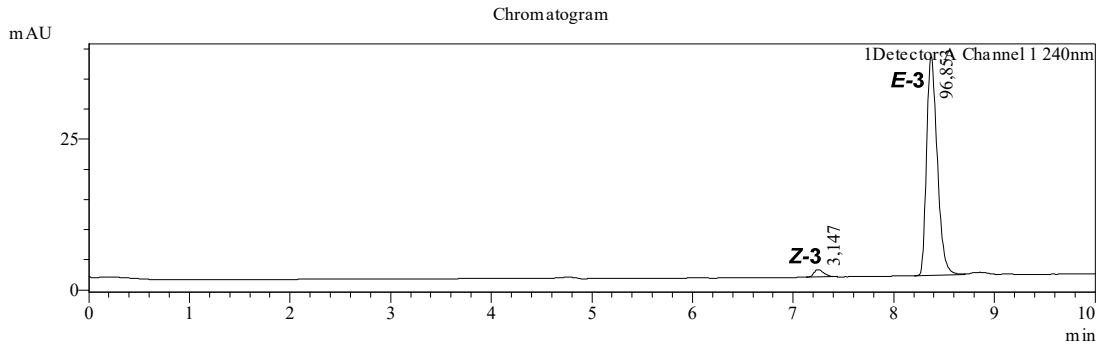
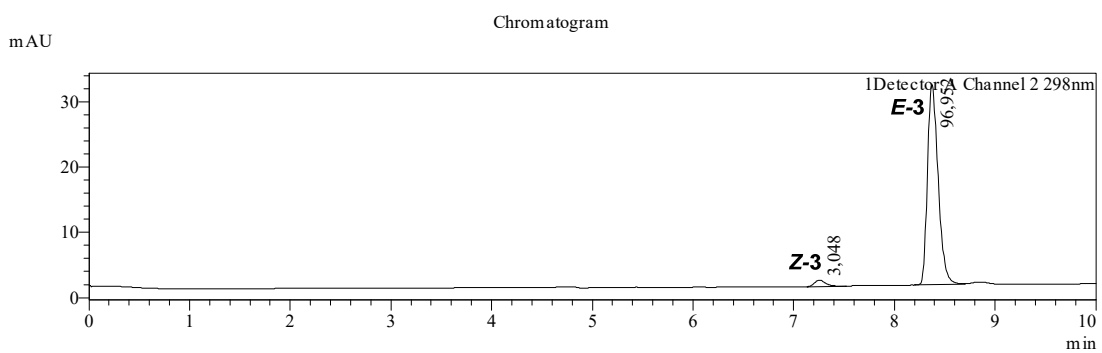
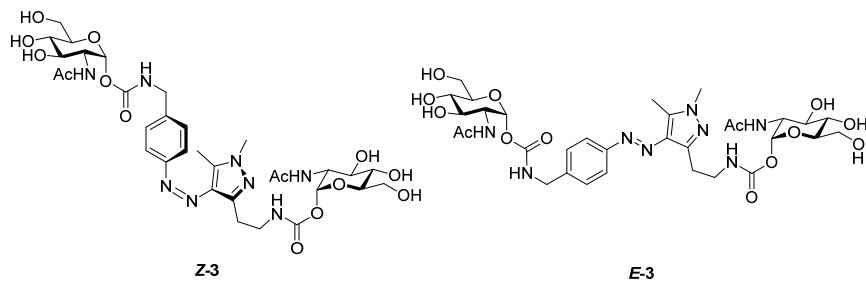
Semi-preparative HPLC profile of **E/Z-11** (65–80% MeCN in 15 min).



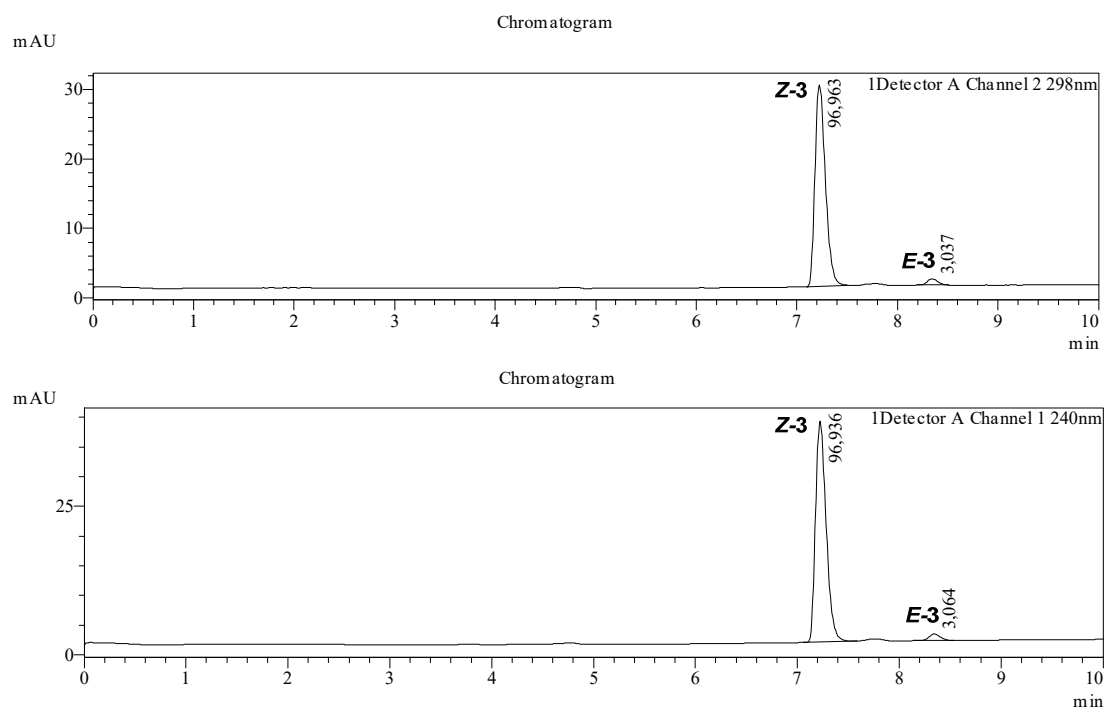
LC-MS profile of purified **E-13** (30–80% MeCN in 10 min).



LC-MS profile of purified **E-3** (10–50% MeCN in 10 min).



Integrated LC-MS profiles of photoligand **3** in PSS (532 nm, 280 mW, 2 min) detected at 298 nm and 240 nm (10–70% MeCN in 10 min).



Integrated LC-MS profiles of photoligand **3** in PSS (355 nm, 50 mW, 2 min) detected at 298 nm and 240 nm (10–70% MeCN in 10 min).

2. Determination of Quantum Yields

Quantum yields have been determined as described earlier.^[1] With the laser power P it is possible to calculate the molar photon flux q_{in} as:

$$q_{\text{in}} = \frac{P\lambda}{hcN_A}$$

with:

q_{in} : Molar photon flux [mol s⁻¹]

P : Power of the laser [W]

λ : Wavelength [m]

h : PLANCK's constant [J s]

c : Speed of light [m s⁻¹]

N_A : AVOGADRO's constant

With the experimental rate constant determined, it is possible to calculate the quantum yield. For an unidirectional photoreaction triggered by monochromatic light, the rate constant can be described as:^[2]

$$r_{A \rightarrow B} = \frac{q_{\text{in}} \Phi_{A \rightarrow B}}{V} (1 - 10^{-\varepsilon_A [A] l})$$

For low absorbances (<<0.43) it can be reformed using a Taylor expansion, from which the linear term is used as an approximate first-order rate constant:

$$r_{A \rightarrow B} = \frac{q_{\text{in}} \Phi_{A \rightarrow B} \varepsilon_A l}{V} [A]$$

This is then rearranged to obtain:

$$\Phi_{A \rightarrow B} = \frac{V t_1}{q_{\text{in}} \varepsilon_A l \ln 10}$$

with:

$\Phi_{A \rightarrow B}$: Quantum yield

t_1 : Experimental rate constant [s⁻¹]

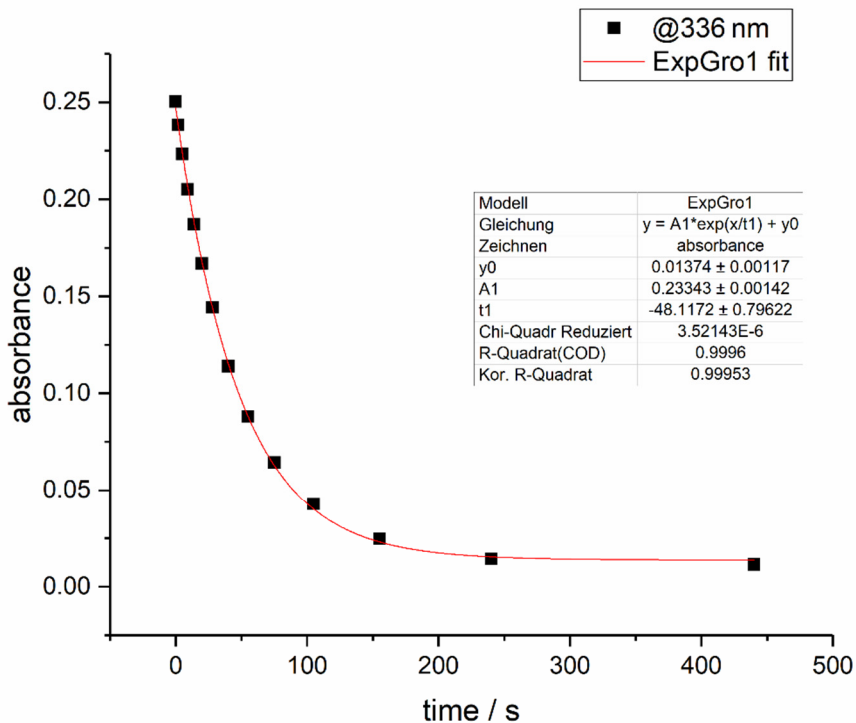
V : Sample volume [mL]

ε_A : Molar extinction coefficient; [M⁻¹ cm⁻¹]

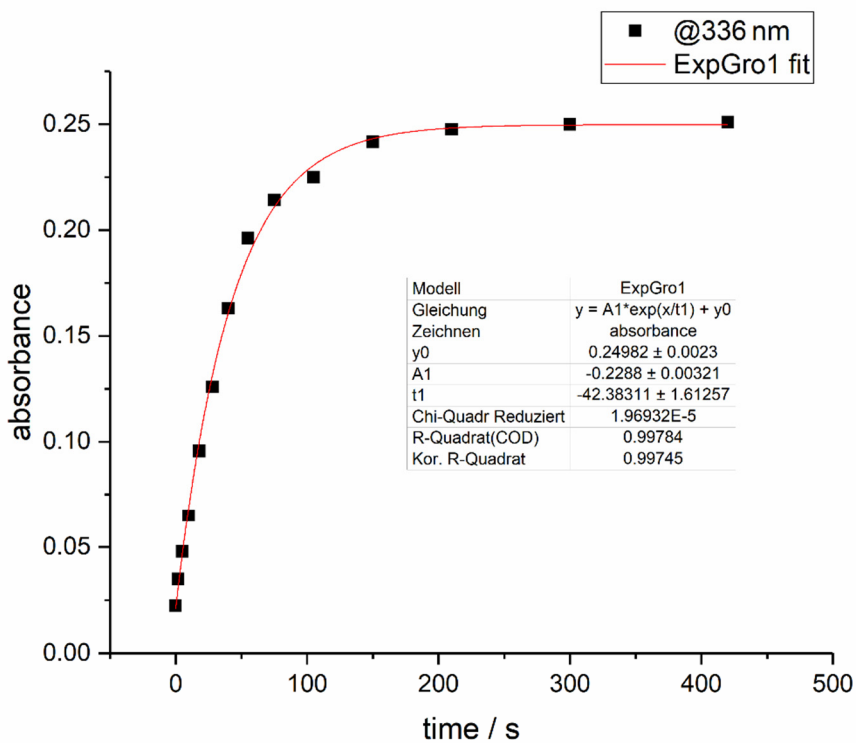
l : Pathlength [cm] (as illuminated from the top: equals filling level of the cuvette: 3.3 cm ± 0.1 cm)

q_{in} : Molar photon flux [mmol s⁻¹]

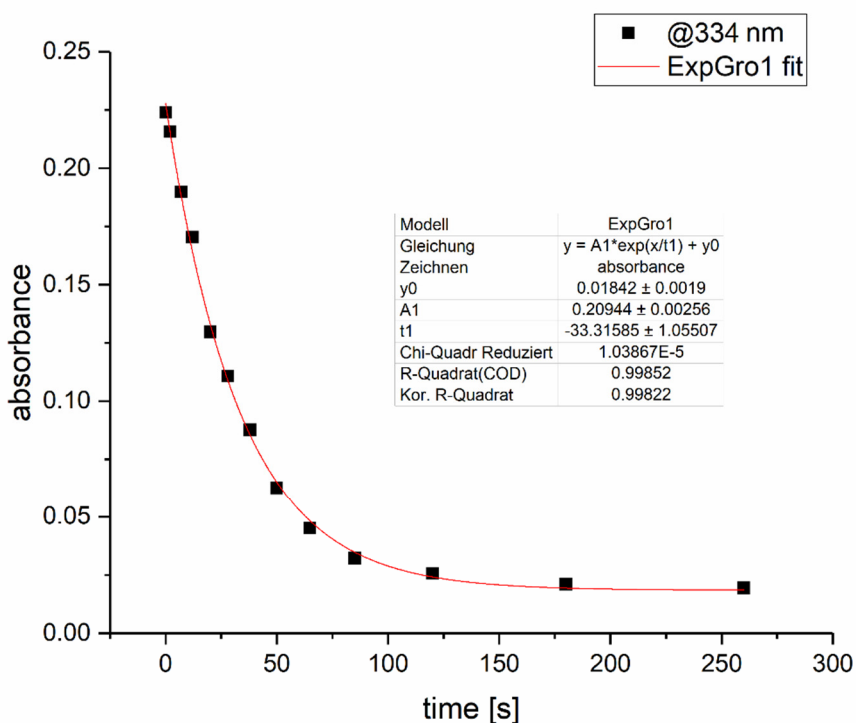
The experimental rate constant t_1 is determined from the irradiation-time dependent absorption change by an exponential fit as shown in the following figures.



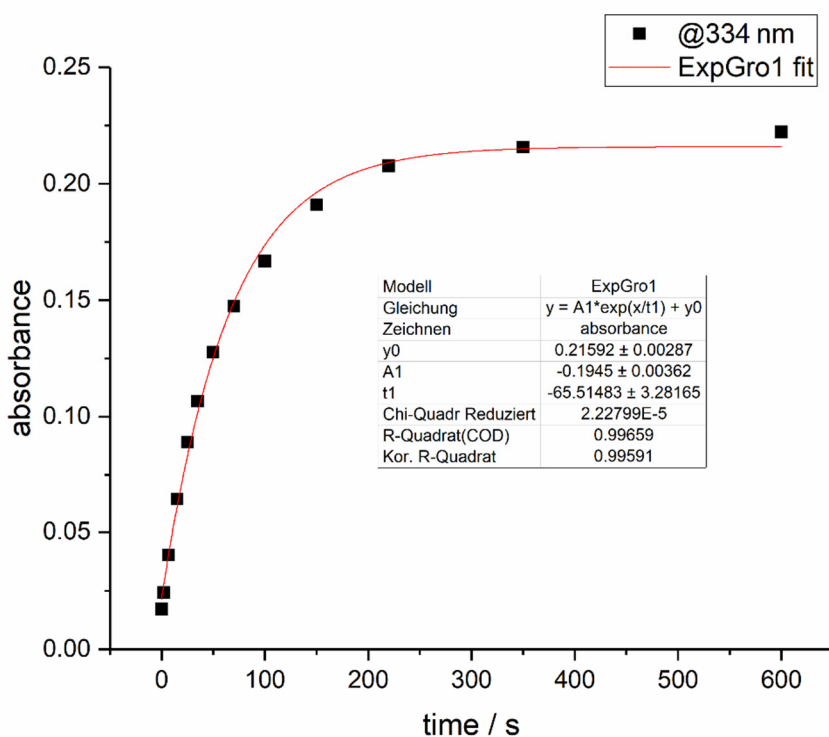
Photoisomerization kinetics (absorbance at 336 nm) of **1** in MeCN upon irradiation at 355 nm (0.0404 ± 0.0017 mJ,^[3] 10 Hz).



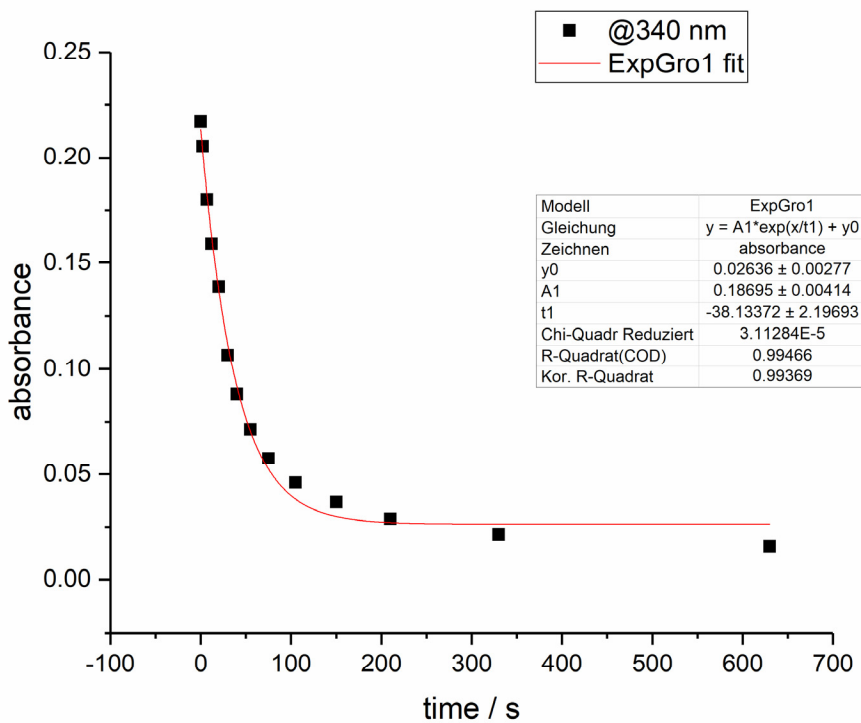
Photoisomerization kinetics (absorbance at 336 nm) of **1** in MeCN upon irradiation at 532 nm (4.35 ± 0.05 mJ, 10 Hz).



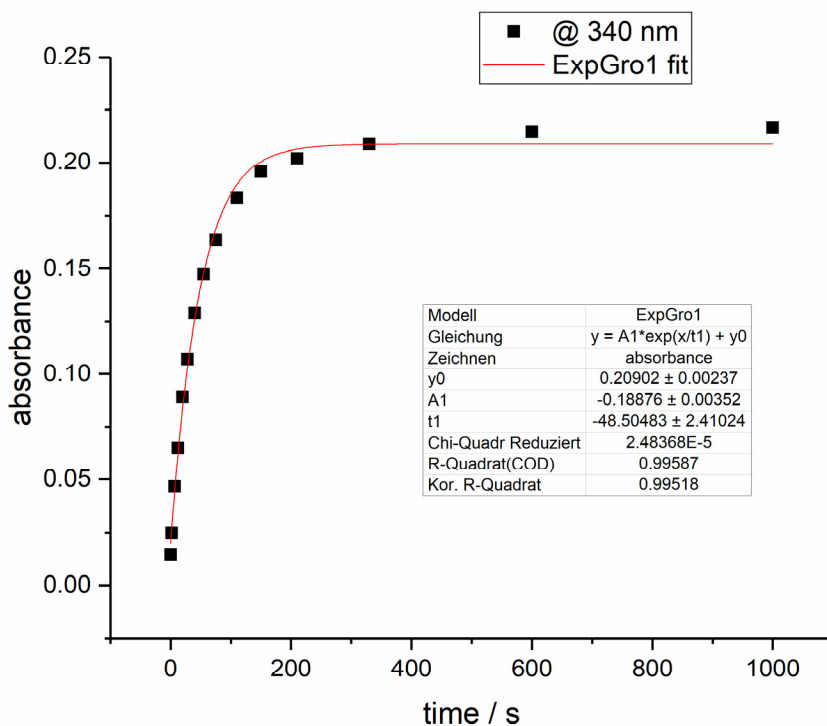
Photoisomerization kinetics (absorbance at 334 nm) of **1** in water upon irradiation at 355 nm (0.042 ± 0.005 mJ,^[3] 10 Hz).



Photoisomerization kinetics (absorbance at 334 nm) of **1** in water upon irradiation at 532 nm (5.2 ± 0.1 mJ, 10 Hz).

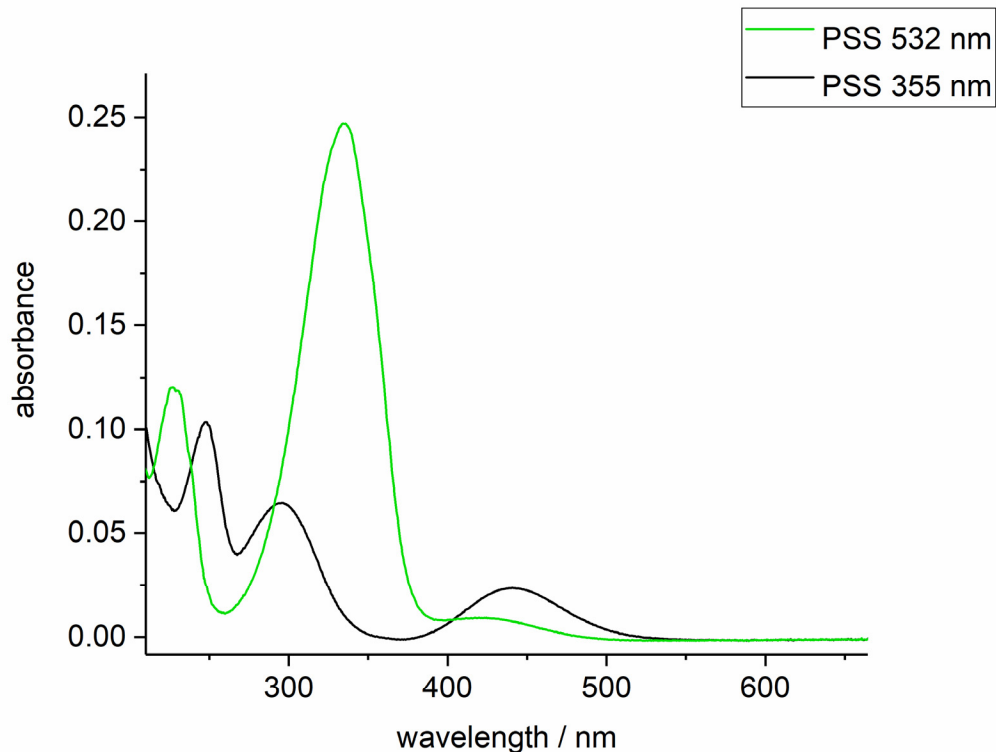


Photoisomerization kinetics (absorbance at 340 nm) of **3** in water upon irradiation at 355 nm (0.0412 ± 0.0017 mJ,^[3] 10 Hz).

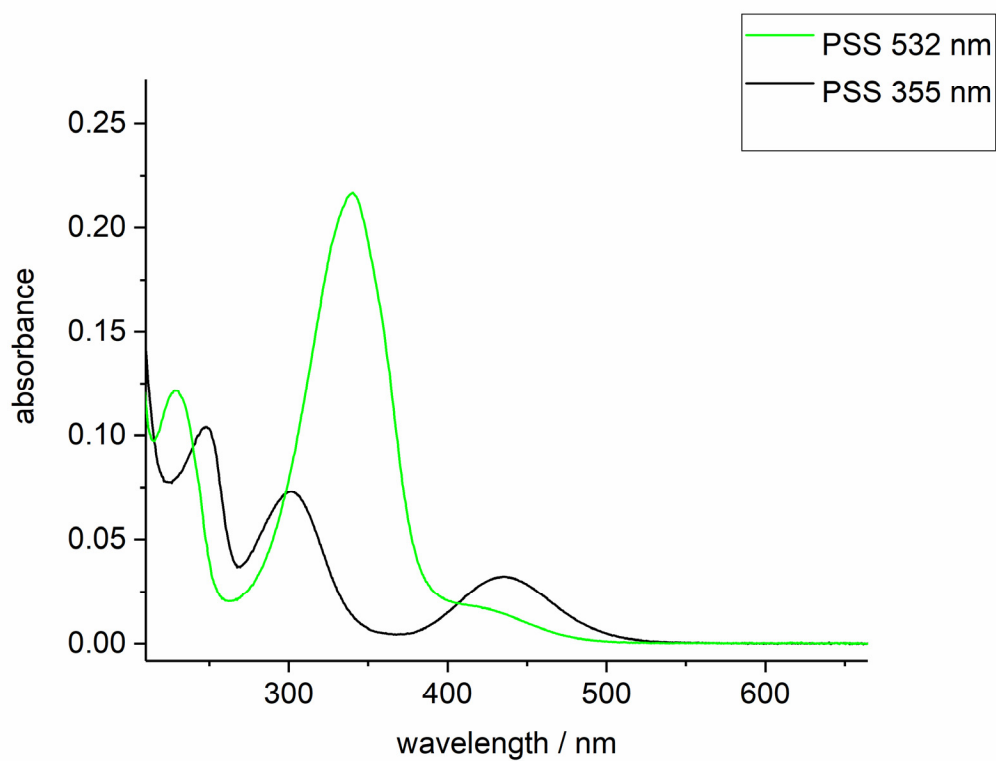
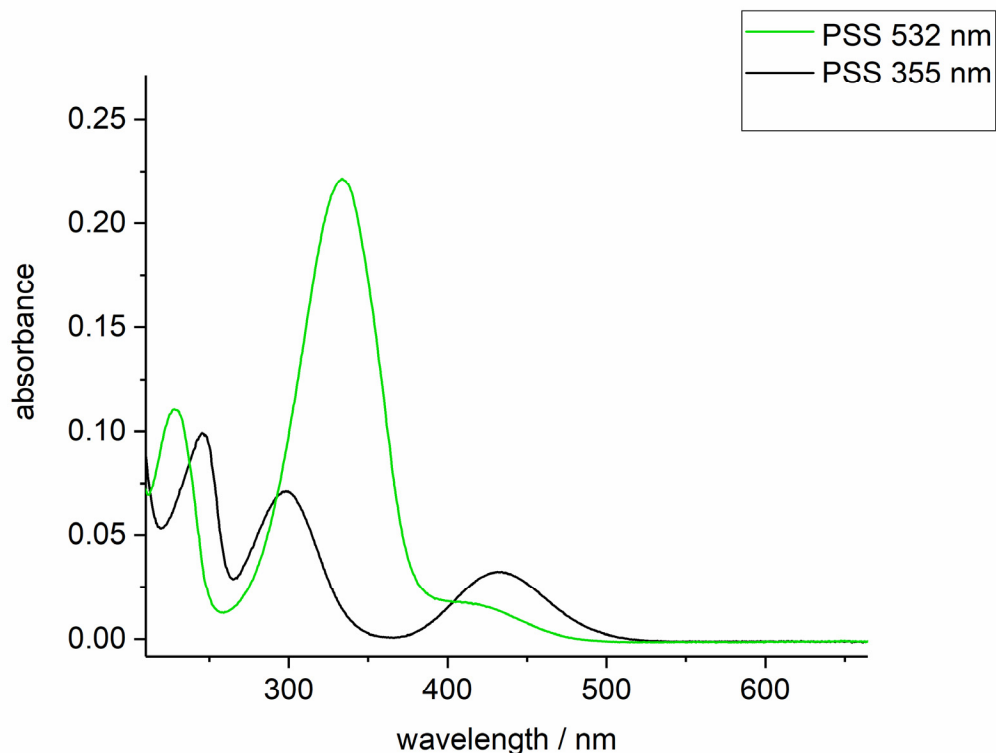


Photoisomerization kinetics (absorbance at 340 nm) of **3** in water upon irradiation at 532 nm (4.45 ± 0.05 mJ, 10 Hz).

Molar extinction coefficients ε_A of the pure isomers at either 355 nm or 532 nm were determined in good approximation from the spectra of compounds in the PSS recorded at a scan rate of 300 nm/min. Error values were calculated by standard propagation of uncertainty.

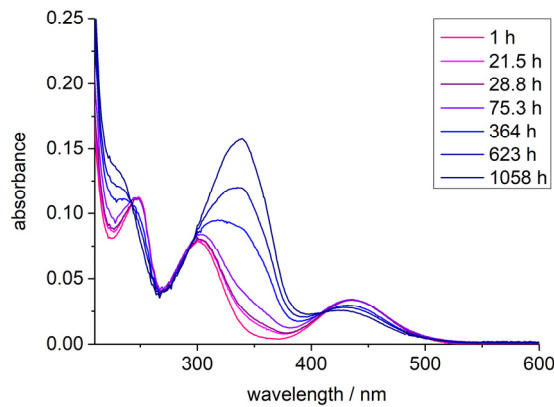


Absorption spectra of **E-1** and **Z-1** in MeCN in PSS. Molar extinction coefficients:
 $\varepsilon^{E-1}_{355\text{ nm}} = 1.48 \cdot 10^5 \text{ M}^{-1}\text{cm}^{-1}$, $\varepsilon^{Z-1}_{532\text{ nm}} = 8.57 \cdot 10^2 \text{ M}^{-1}\text{cm}^{-1}$



3. Determination of Thermal Half-Life

For determination of the thermal half-life $t_{1/2}$, a 1.4 mL Suprasil cuvette type 114-QS from Hellma Analytics was filled with 1 mL of aqueous solution of photoligand **3**, brought into PSS (355 nm, 50 mW, 2 min), and sealed with a Teflon stopper. The sample of **Z-3** was then kept in the dark at 20 °C and UV/vis spectra were measured over time as described in the general methods. The number of scans was kept low to minimize the influence of the UV/vis measuring beam. The background absorbance of the cuvette filled with water was automatically subtracted from each measurement.



UV/vis spectra depicting the relaxation of **Z-3** over time at 20 °C.

As the concentration is linked linear to the absorption by the LAMBERT-BEER-Law, the absorption at the maximum (339 nm) was used to calculate the percentage of Z isomer as follows:

$$E_t - E_0 = E_t^\Delta$$

$$\frac{E_\infty^\Delta - E_t^\Delta}{E_\infty^\Delta} = N_t^Z$$

with:

E_0 : Absorption of Z isomer

E_t : Absorption measured at time t

E_∞^Δ : Absorption difference of E isomer and Z isomer.

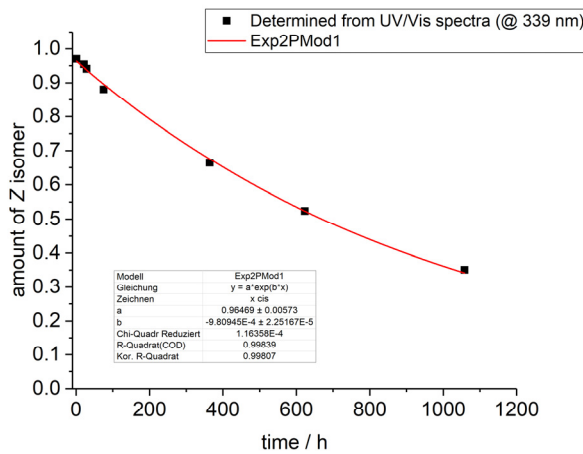
E_t^Δ : Absorption difference at time t

N_t^Z : percentage of Z isomer at time t

Assuming 1st order kinetics, the percentage of Z isomer N_t^Z can then be plotted against t and fitted with an exponential decay:

$$N_t^Z = N_0^Z \cdot e^{bt}$$

with b as exponential thermal relaxation constant.



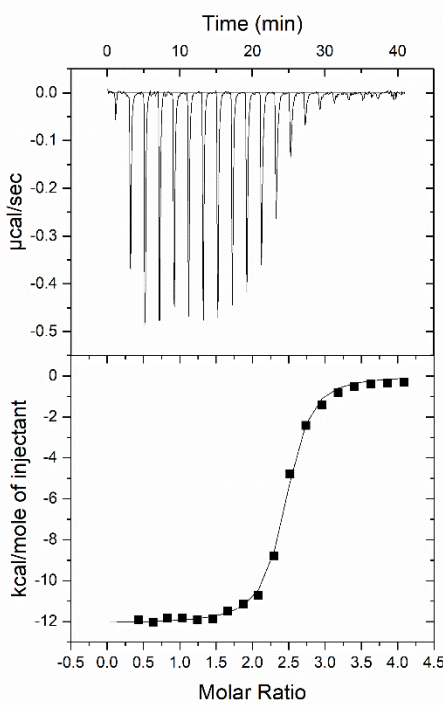
Percentage of Z isomer of photoligand **3** in the dark at 20 °C (determined from the absorbance at 339 nm) over time and exponential decay fit.

The half-life of a first order kinetic is then given as:

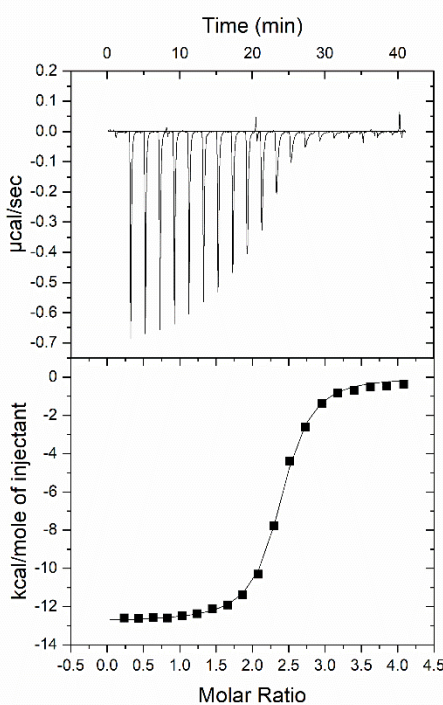
$$t_{1/2} = \frac{\ln(2)}{b}$$

Error value was calculated by standard propagation of uncertainty.

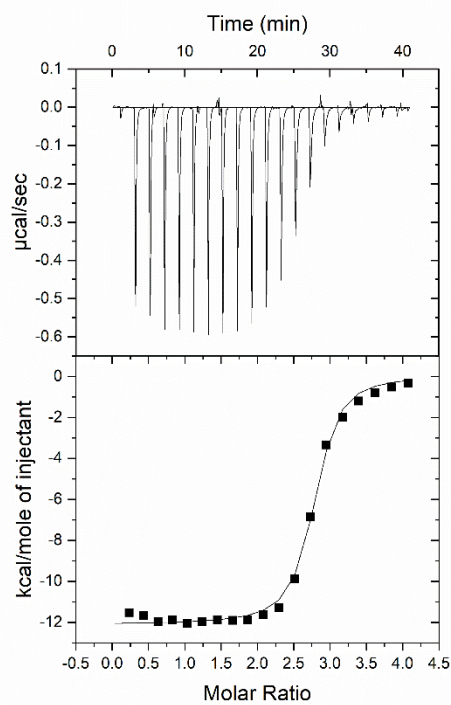
4. ITC Experiments



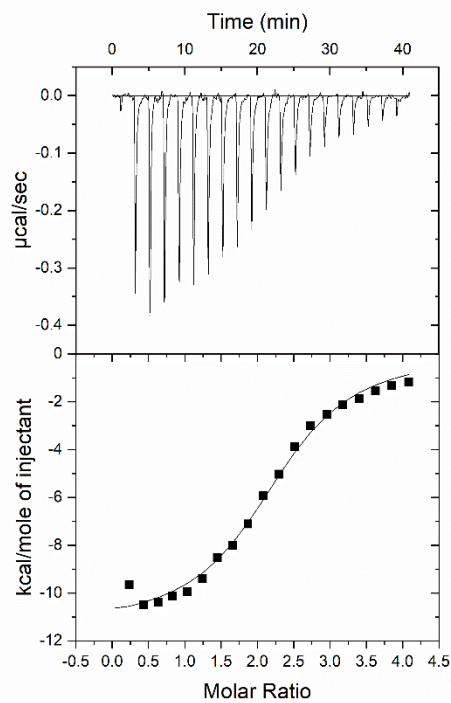
Thermogram 1 of **E-3** ($[\text{WGA}] = 14.2 \mu\text{M}$, $[\text{E-3}] = 284.3 \mu\text{M}$).



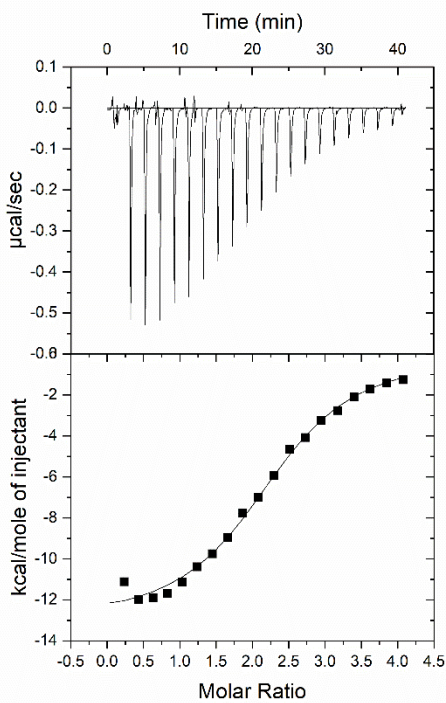
Thermogram 2 of **E-3** ($[\text{WGA}] = 15.1 \mu\text{M}$, $[\text{E-3}] = 302.3 \mu\text{M}$).



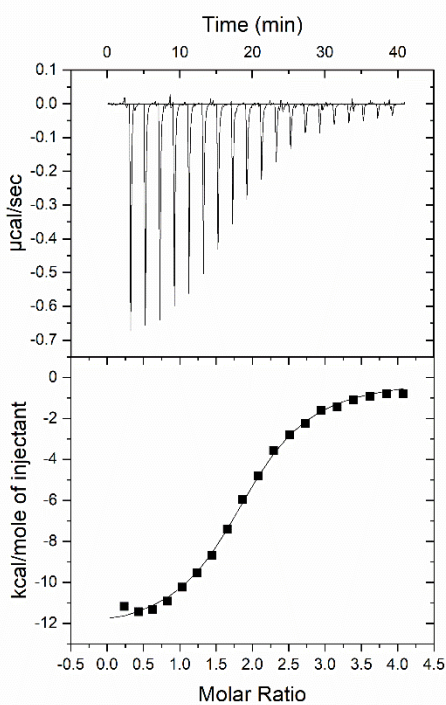
Thermogram 3 of **E-3** ($[\text{WGA}] = 14.6 \mu\text{M}$, $[\text{E-3}] = 292.0 \mu\text{M}$).



Thermogram 1 of **Z-3** ($[\text{WGA}] = 14.2 \mu\text{M}$, $[\text{Z-3}] = 284.3 \mu\text{M}$).



Thermogram 2 of **Z-3** ([WGA] = 17.7 μM , [Z-3] = 353.6 μM).



Thermogram 3 of **Z-3** ([WGA] = 13.3 μM , [Z-3] = 266.1 μM).

Binding Equilibria with two Ligands

Basic relations

Since ligand **3** after irradiation with light of either 532 nm or 355 nm exists in a PSS of *E* and *Z* isomers containing 3% of the minor isomer, and since both isomers have different binding affinities to WGA, we treat the combined binding equilibria and pertinent ITC experiments with mixtures of the isomers in a quantitative manner. We adopt notations analogous to those used by Wiseman et al.^[4] for deriving the ITC curve in case of a single ligand.

X_E	unbound <i>E</i> isomer of ligand
X_Z	unbound <i>Z</i> isomer of ligand
X_{tot}	total concentration of ligands
α	fraction of <i>E</i> isomer in X_{tot}
M	unbound lectin WGA
M_{tot}	total concentration of WGA binding sites (i.e., pairs of primary binding sites)
MX_E	single pair of binding sites occupied by X_E
MX_Z	single pair of binding sites occupied by X_Z
$K_{a,E}$	association constant of <i>E</i> isomer
$K_{a,Z}$	association constant of <i>Z</i> isomer

Concentrations are indicated by square brackets.

The following equations serve to calculate the concentrations of the unbound ligand isomers in solution, whereby we assume that there are two pairs of ligand binding sites on each WGA molecule, the latter being expressed by the factor 2 in eq. (1e).

$$\begin{aligned} [MX_E] &= K_{a,E}[X_E][M] \\ [MX_Z] &= K_{a,Z}[X_Z][M] \\ [X_E] + [MX_E] &= \alpha[X_{tot}] \\ [X_Z] + [MX_Z] &= (1 - \alpha)[X_{tot}] \\ [M] + [MX_E] + [MX_Z] &= 2[M_{tot}] \end{aligned} \quad (1 \text{ a-e})$$

The last three equations (1c-e) can be used to eliminate the variables referring to the unbound species $[X_E]$, $[X_Z]$, and $[M]$ leaving us with two equations for the concentrations of the bound species MX_E and MX_Z .

$$\begin{aligned} [MX_E] &= K_{a,E}(2M_{tot} - [MX_E] - [MX_Z])(\alpha X_{tot} - [MX_E]) \\ [MX_Z] &= K_{a,Z}(2M_{tot} - [MX_E] - [MX_Z])(1 - \alpha)X_{tot} - [MX_Z]) \end{aligned} \quad (2 \text{ a,b})$$

At this point, we convert equations (2 a,b) into dimensionless equations by dividing both sides of each equation by M_{tot} and introducing the following dimensionless quantities (eq. 3 a-e).

$$\begin{aligned}
 c_E &= K_{a,E} M_{tot} \\
 c_Z &= K_{a,Z} M_{tot} \\
 x &= X_{tot} / M_{tot} \\
 y_E &= [MX_E] / M_{tot} \\
 y_Z &= [MX_Z] / M_{tot}
 \end{aligned} \tag{3 a-e}$$

This procedure yields:

$$\begin{aligned}
 y_E &= c_E (2 - y_E - y_Z)(\alpha x - y_E) \\
 y_Z &= c_Z (2 - y_E - y_Z)((1-\alpha)x - y_Z)
 \end{aligned} \tag{4 a,b}$$

These equations are solved for y_E and y_Z as functions of the titration variable x using the *Mathematica* software package.^[5] For each of these variables, two solutions are obtained. The titration curve representing the heat release of molar binding as a function of x is obtained by the derivative of the smaller value of the sum of the solutions for y_E and y_Z , multiplied by the molar standard enthalpy of ligation ΔH° . The latter is known from fitting the amplitudes of the theoretical to the experimental curves.

$$Q(x) = \Delta H^\circ d(\text{Min}[y_E(x) + y_Z(x)]) / dx \tag{5}$$

Results

The calculations are based on the following values for the dissociation constants and pertinent association constants with their respective error margins (μM concentration units are used everywhere):

$$\begin{array}{ll}
 K_{d,E} = 0.177 \pm 0.053 & K_{d,Z} = 2.21 \pm 0.08 \\
 K_{a,E} = 5.65 \pm 1.7 & K_{a,Z} = 0.45 \pm 0.016
 \end{array}$$

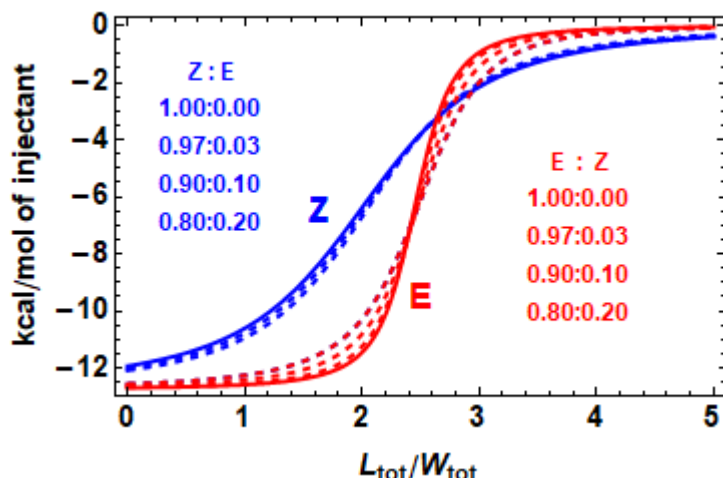


Figure S1. ITC curves calculated for different mixtures of *E* and *Z* isomers. Set of red curves starting with pure *E* isomer, set of blue curves starting with pure *Z* isomer.

Figure S1 shows the calculated ITC curves of pure *E* and *Z* isomers together with the curves obtained upon small admixtures of the other isomer. For the *Z* isomer (with the weaker binding), the effects of the same percentual admixture are smaller than for the *E* isomer (with the stronger binding). An admixture of 3% of the *E* isomer into the *Z* isomer is hardly detectable as a difference in the ITC curve, whereas it makes a small but detectable difference for a corresponding admixture of the *Z* isomer into the *E* isomer.

In Figure S2, two bounding ITC curves corresponding to the error margins of the dissociation constants are drawn together with the curve for the central K_d value in each case. In case of the *E* isomer, there is a little gap between the bounding ITC curves, but the curve calculated for a 97:3 *E/Z* mixture is fully included within these bounds. This means that the uncertainty of K_d with respect to the admixture of the *Z* isomer to the *E* isomer is fully within the error bounds of K_d . In case of the *Z* isomer, there is no gap between the curves representing the error bounds, and the ITC curve calculated for a 3:97 *E/Z* mixture coincides with these.

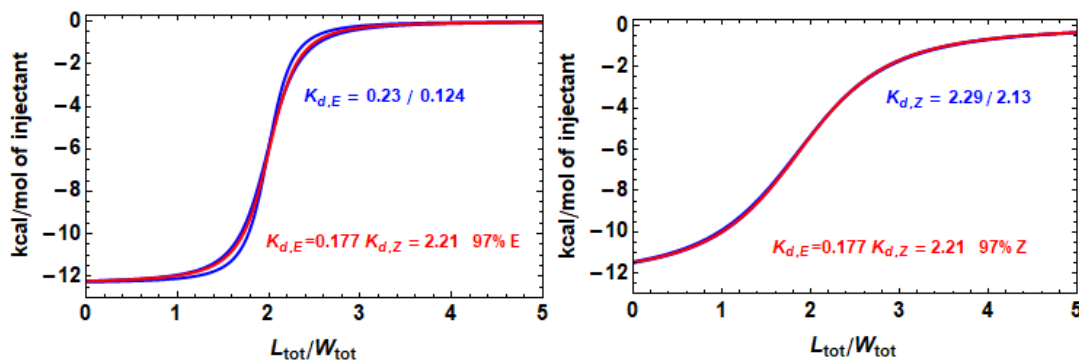
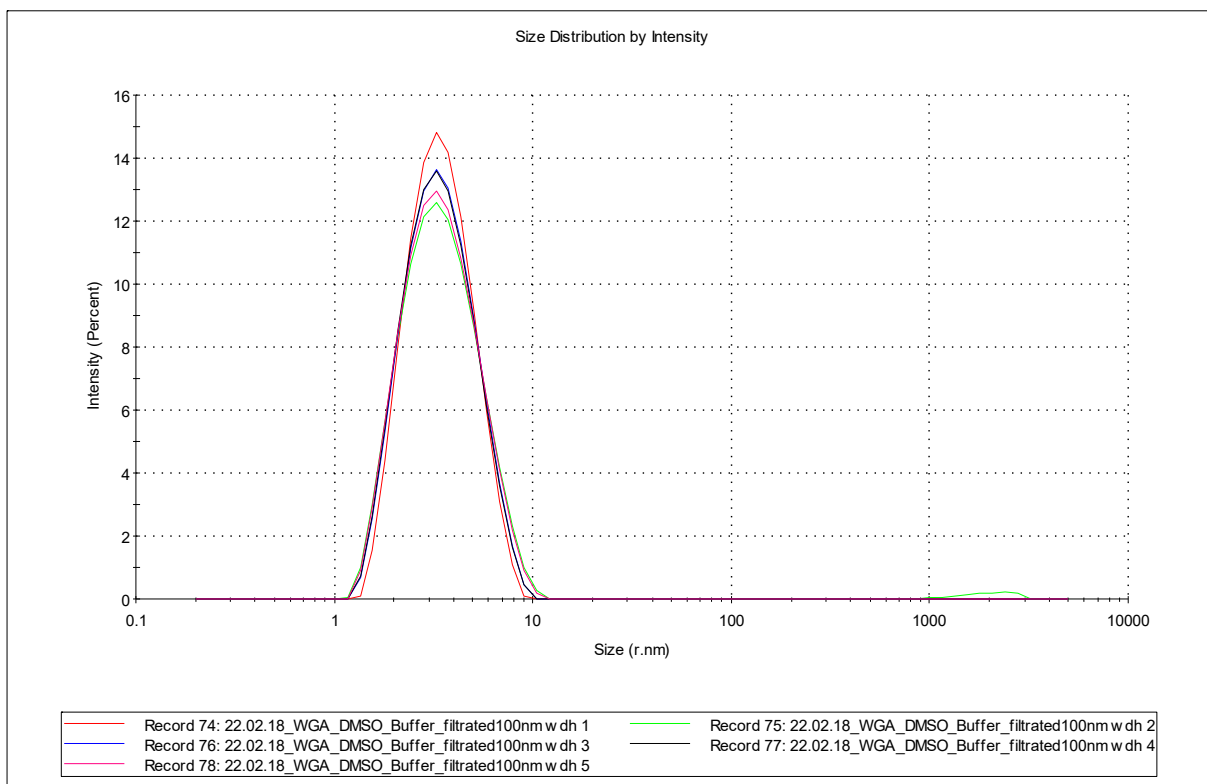
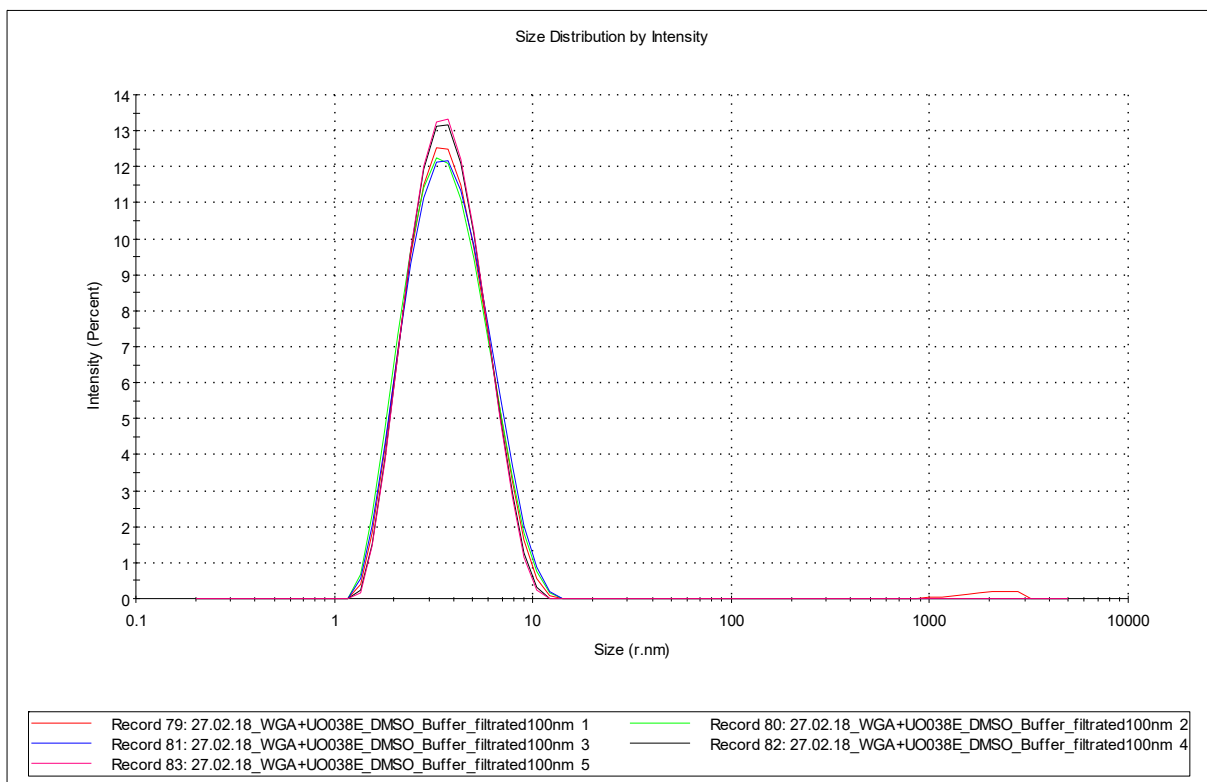


Figure S2. Calculated ITC curves corresponding to the error limits of $K_{d,E}$ (left) and $K_{d,Z}$ (right) for pure isomers (blue) and for mixtures of 97:3 *E/Z* (left) and *Z/E* (right) with the determined values of K_d .

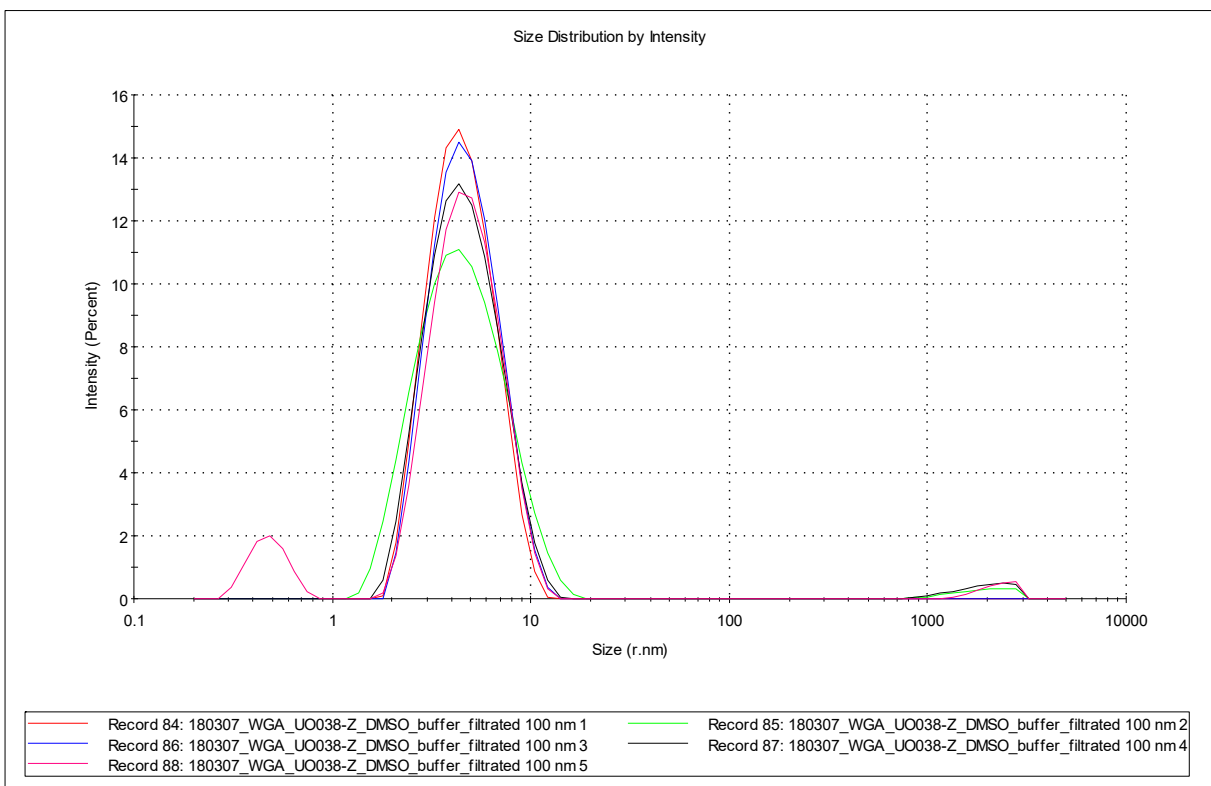
5. DLS Data



Distribution of hydrodynamic radii r determined by DLS of a pure WGA solution.

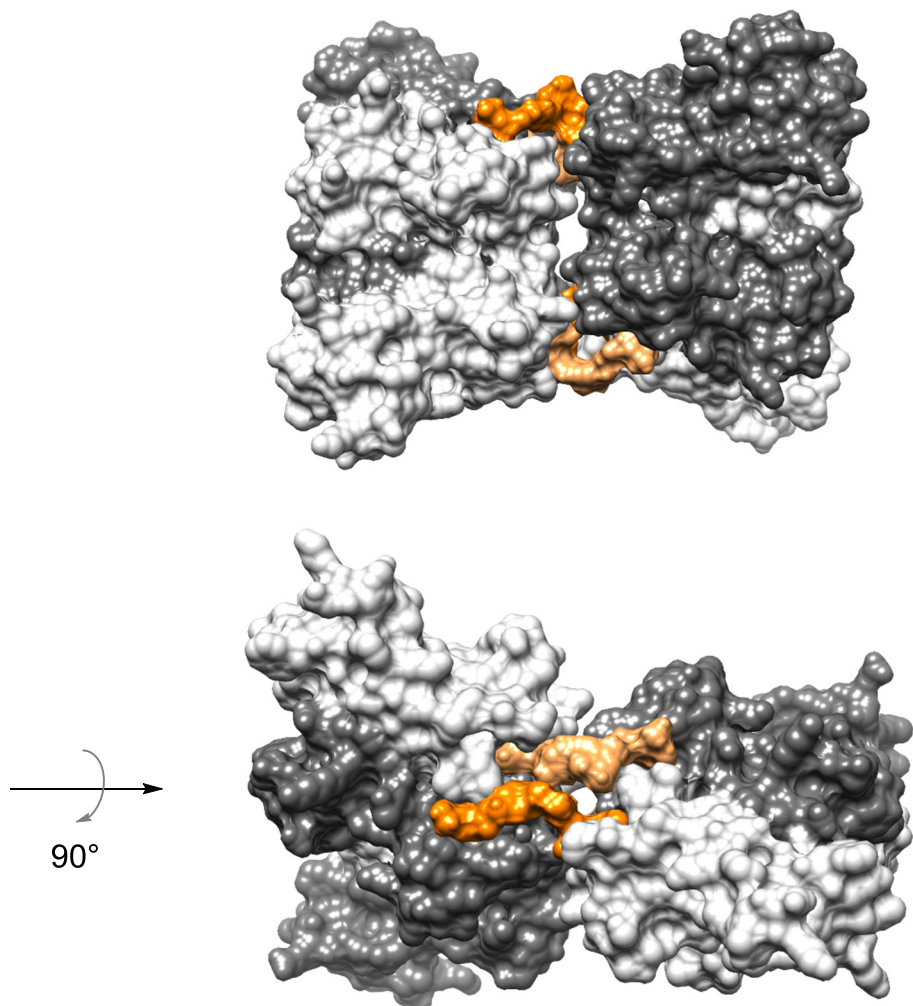


Distribution of hydrodynamic radii r determined by DLS of a solution of WGA and two equivalents of **E-3**.



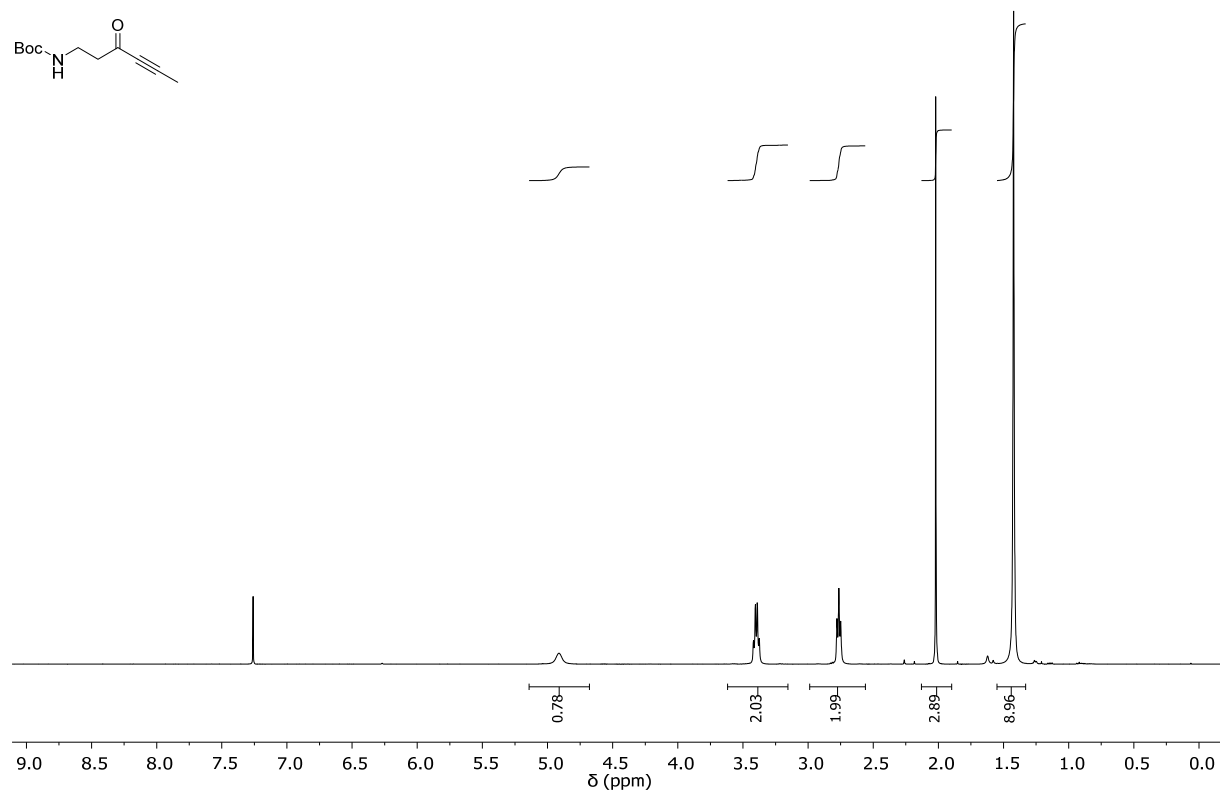
Distribution of hydrodynamic radii r determined by DLS of a solution of WGA and two equivalents of **Z-3**.

6. Possible Structure of WGA in Complex with Z-3

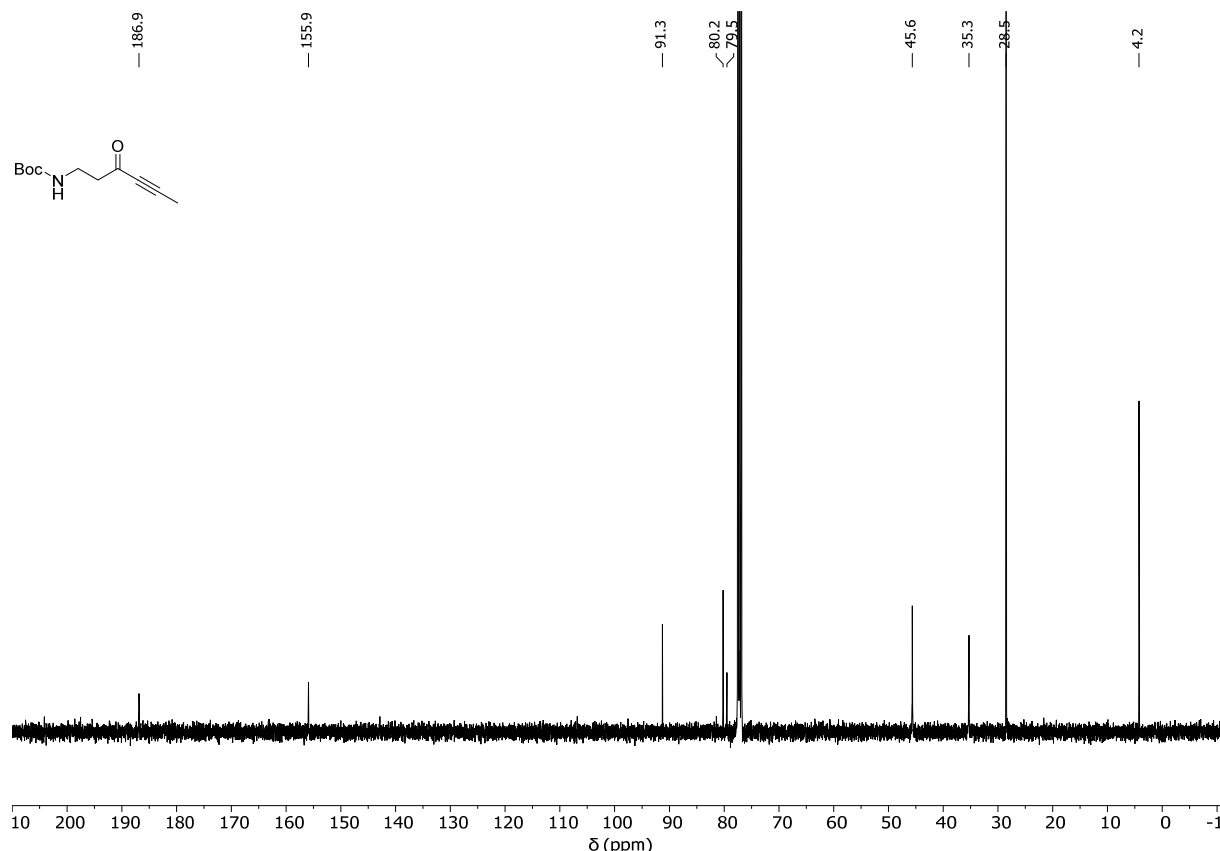


A possible cross-linked species of WGA (subunits in light and dark grey) in complex with photoligand **Z-3** (orange and light orange) with 2:4 stoichiometry. The model was generated by manual assembly of protein crystal structures and energetically optimized 3D structure of photoligand **Z-3** (with single bond angles manually adjusted). Carbohydrate moieties of **Z-3** were superimposed with those of a co-crystallized ligand (PDB code 2X52) in all binding pockets.

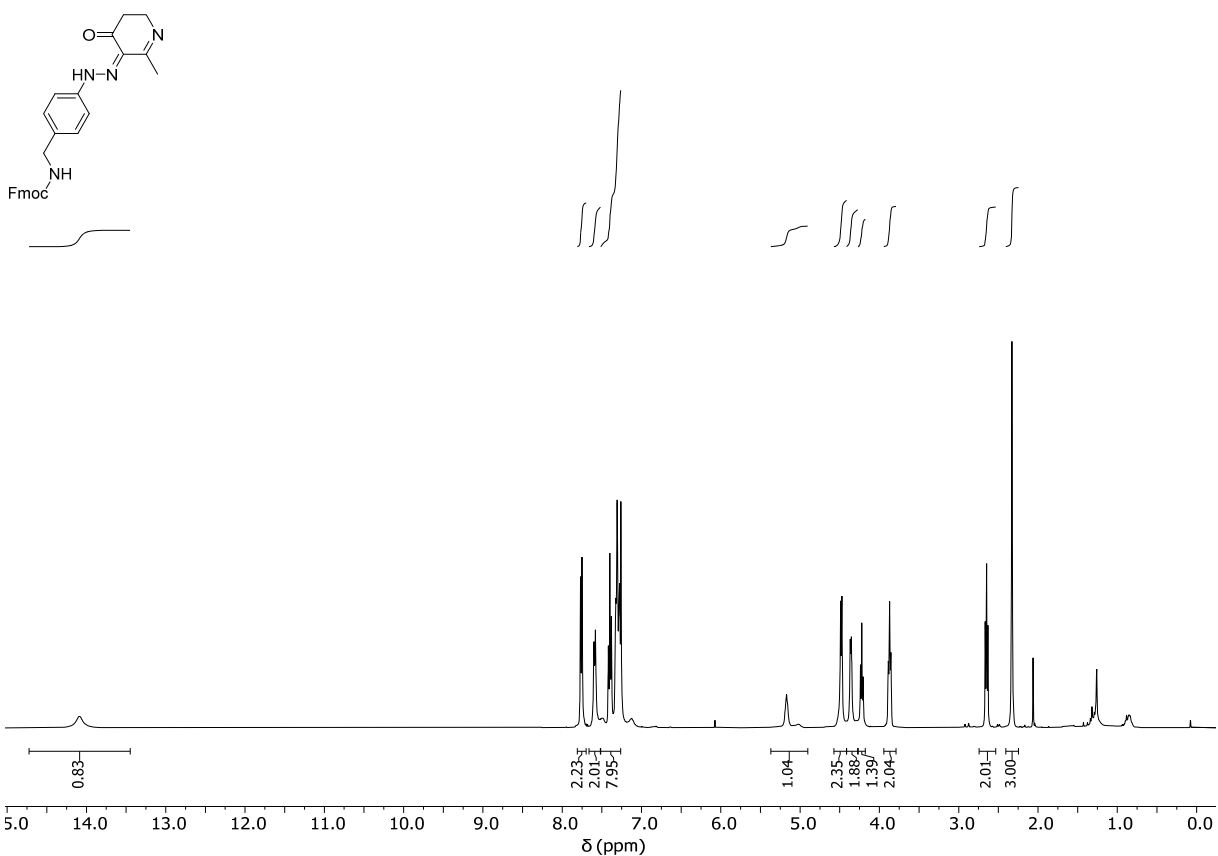
7. NMR Spectra



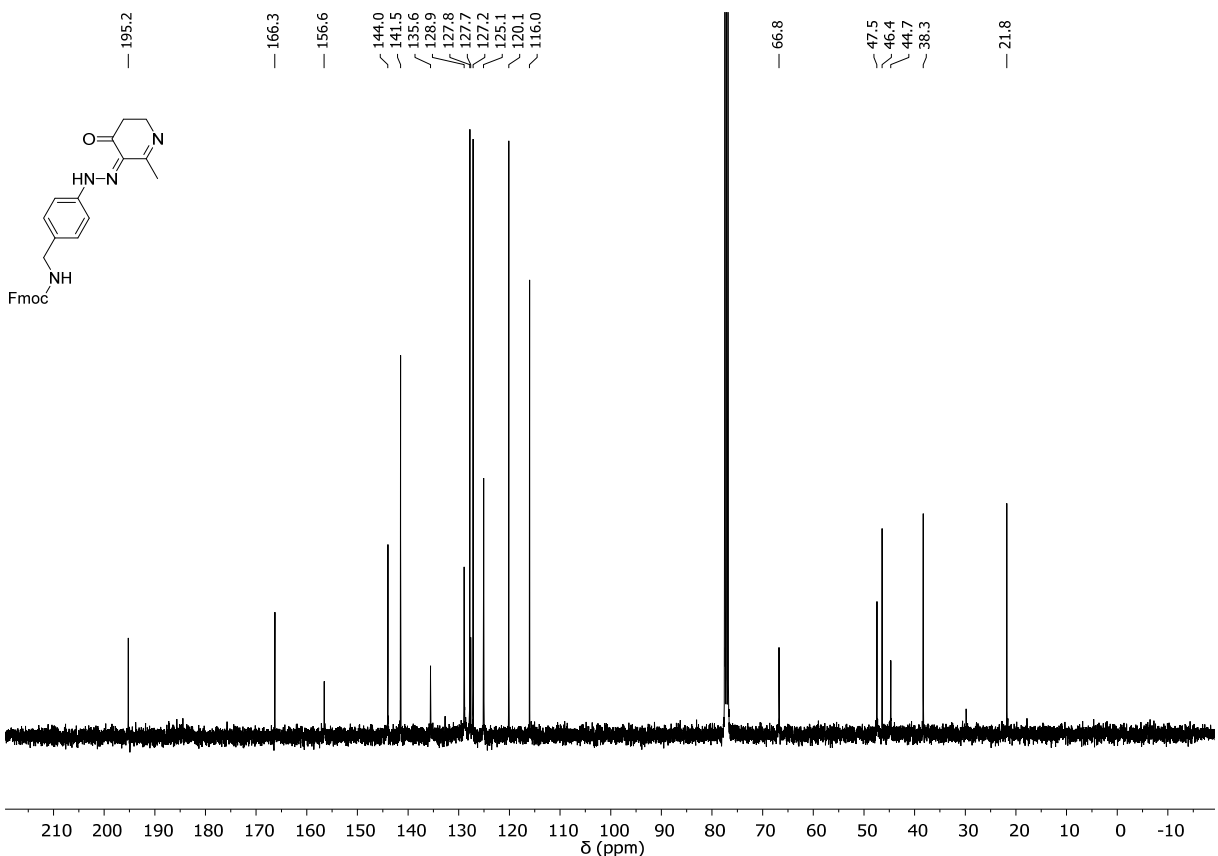
¹H NMR of 5 (CDCl₃, 400 MHz, 300 K).



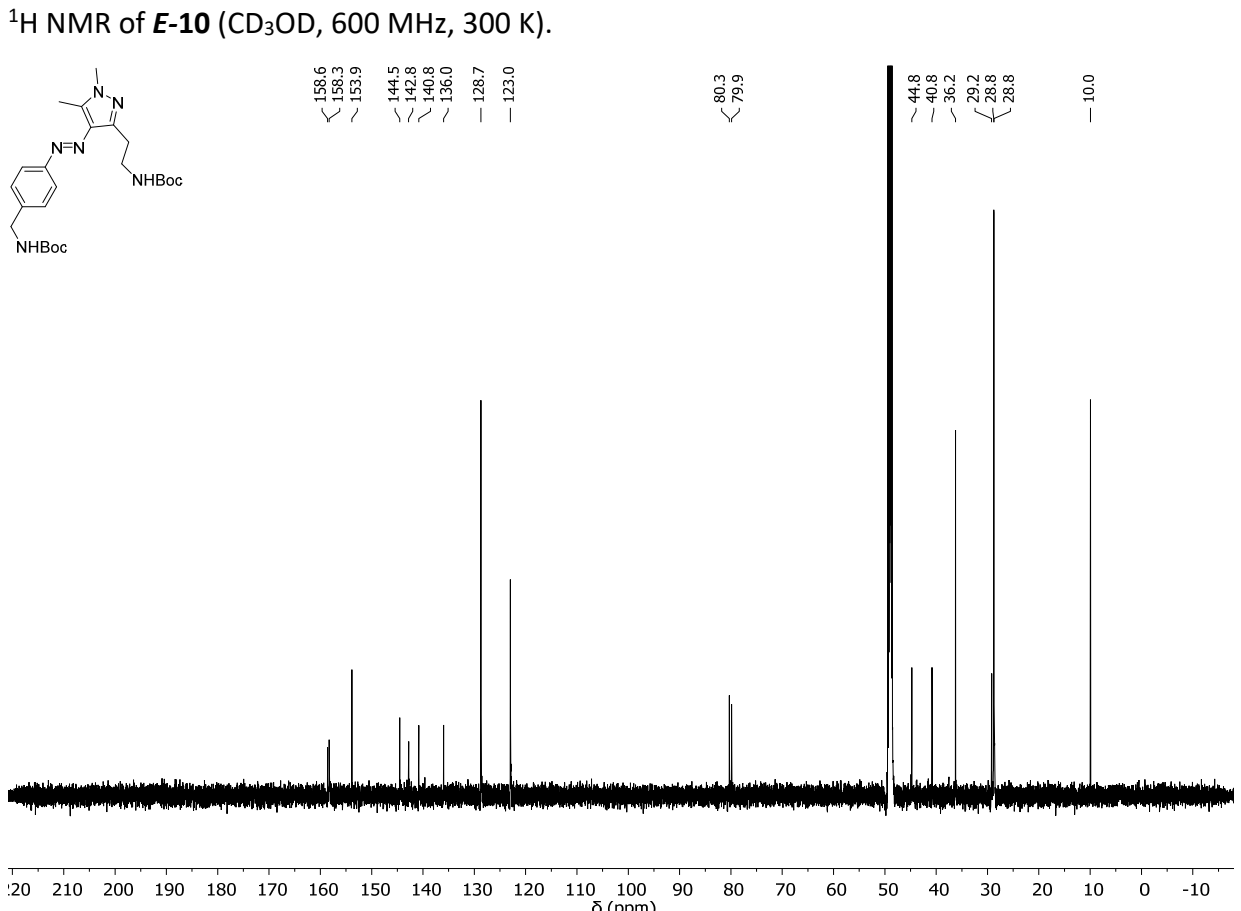
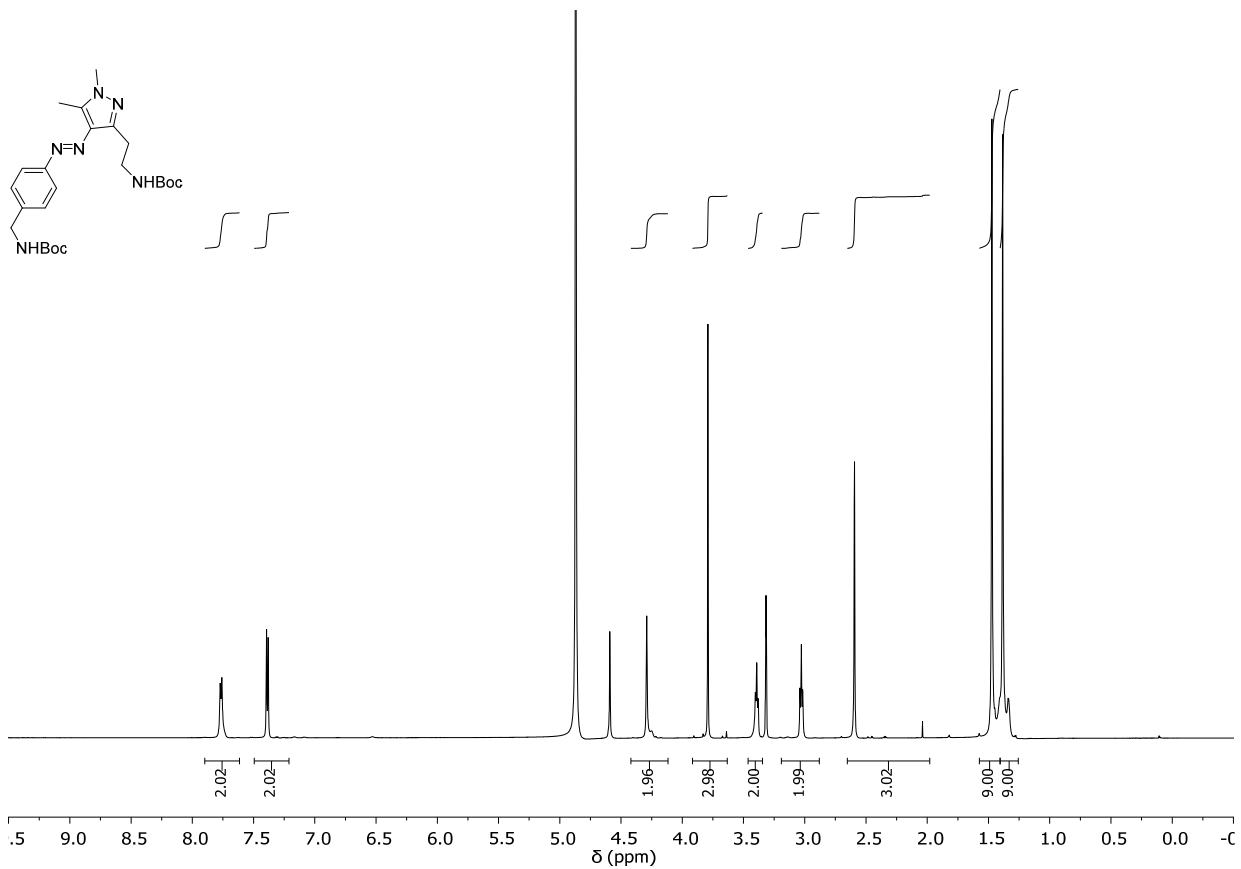
¹³C NMR of 5 (CDCl₃, 101 MHz, 300 K).

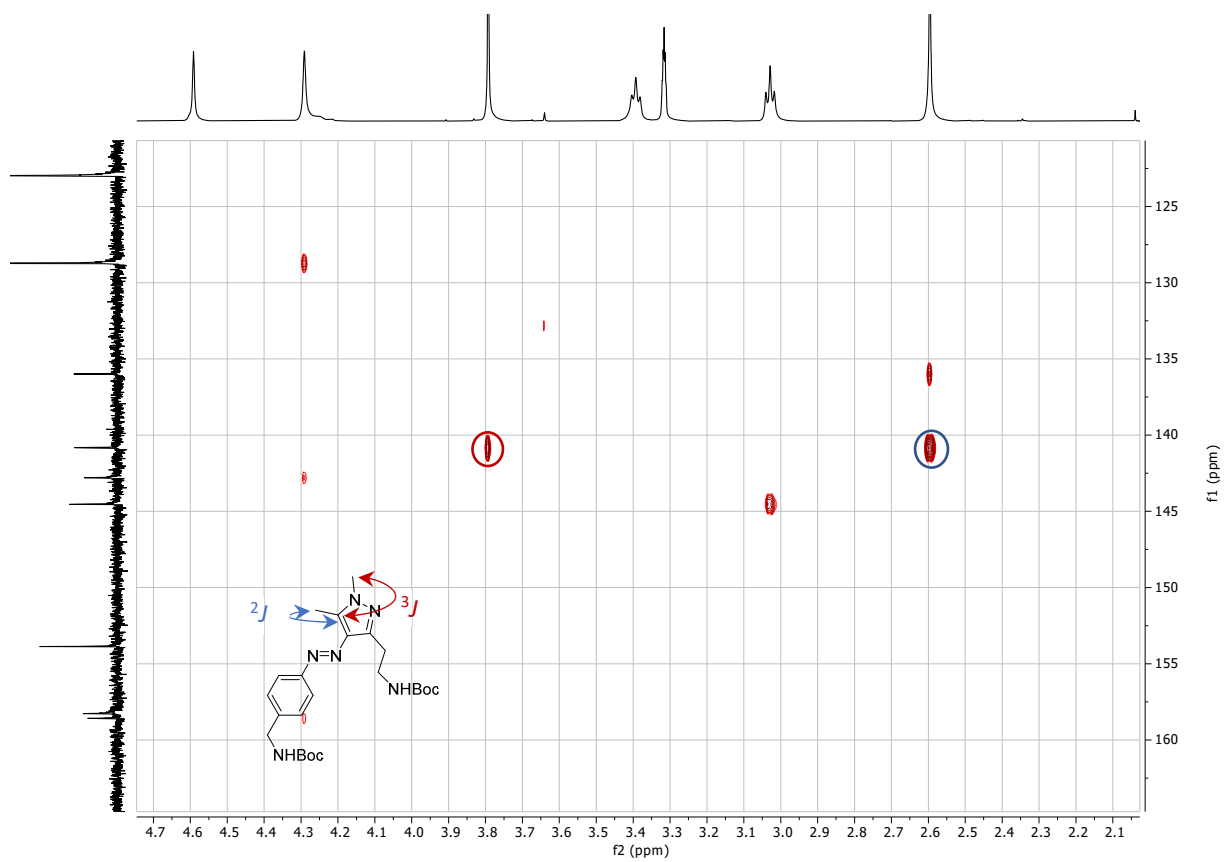


¹H NMR of **9** (CDCl_3 , 400 MHz, 300 K).

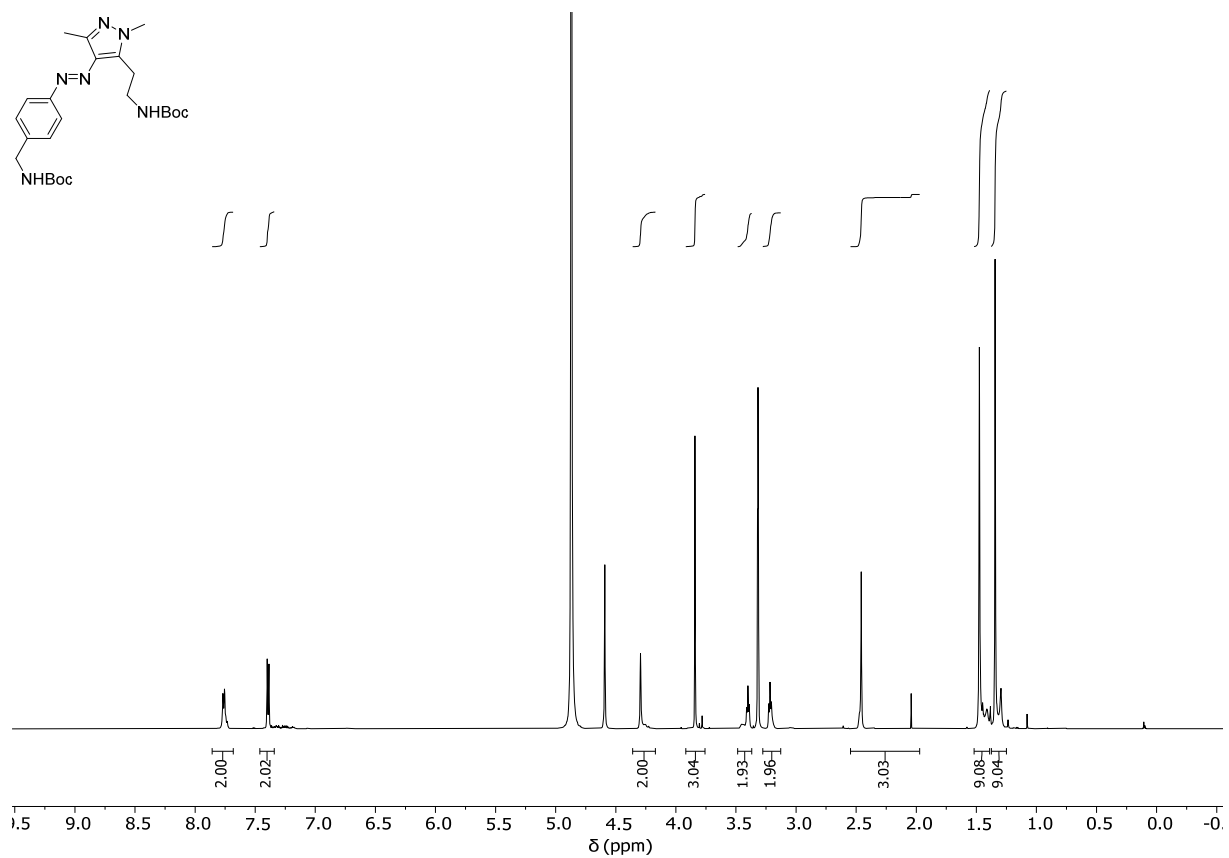


¹³C NMR of **9** (CDCl_3 , 100 MHz, 300 K).

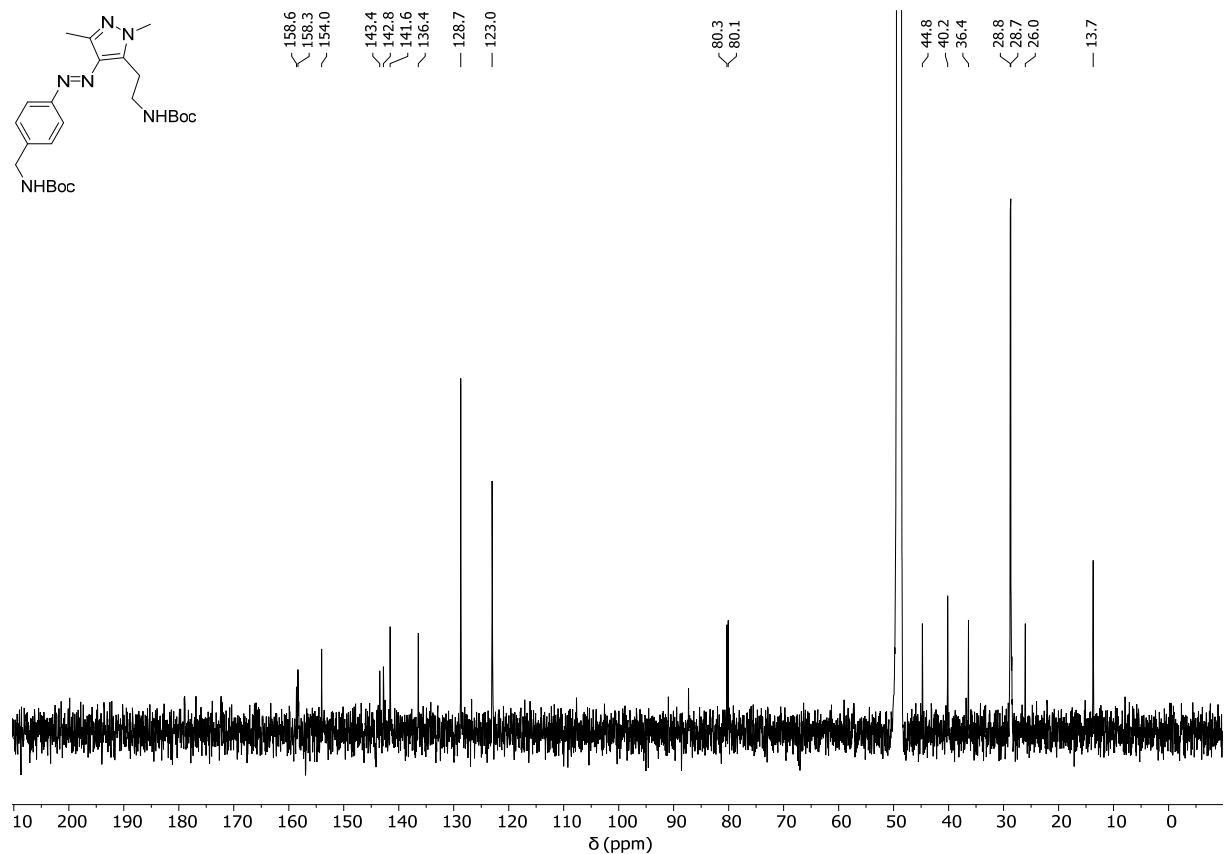




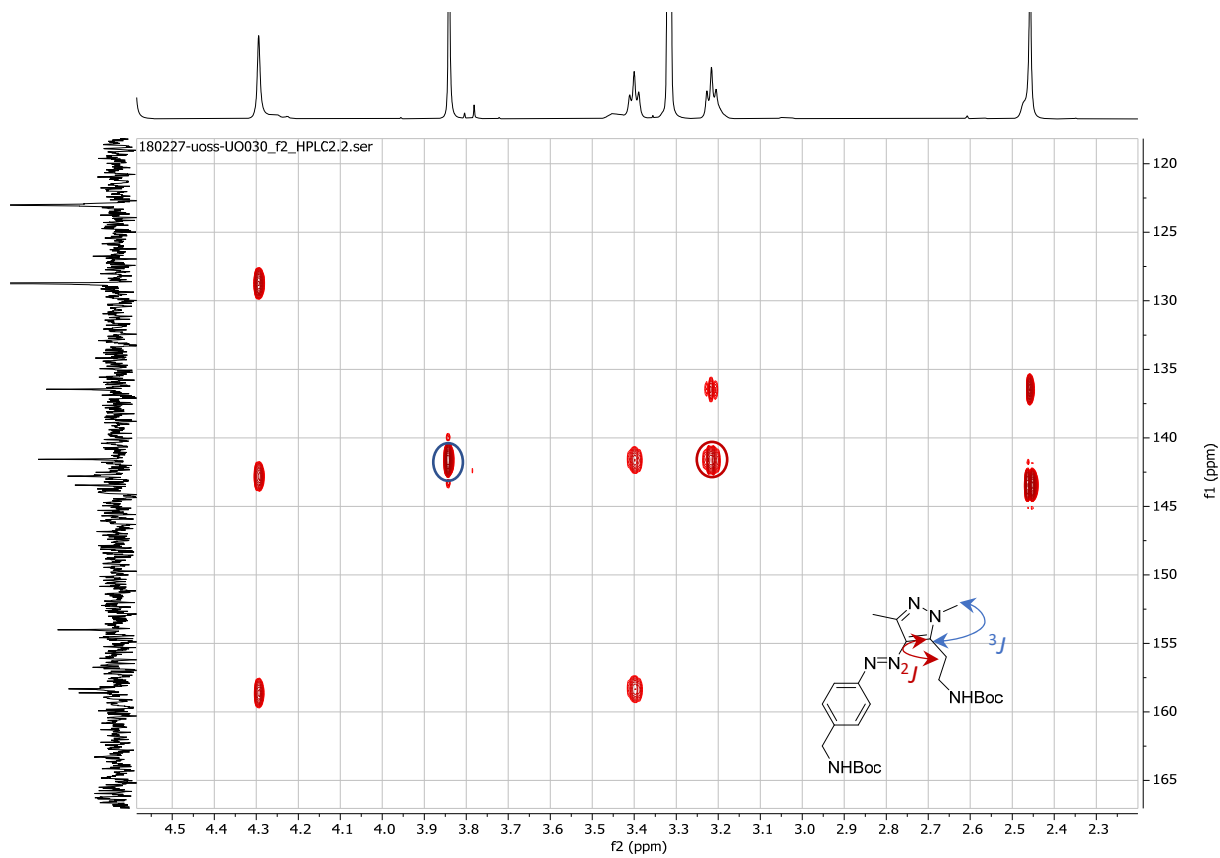
Section of HMBC NMR of **E-10** (CD_3OD , 600 MHz, 300 K).



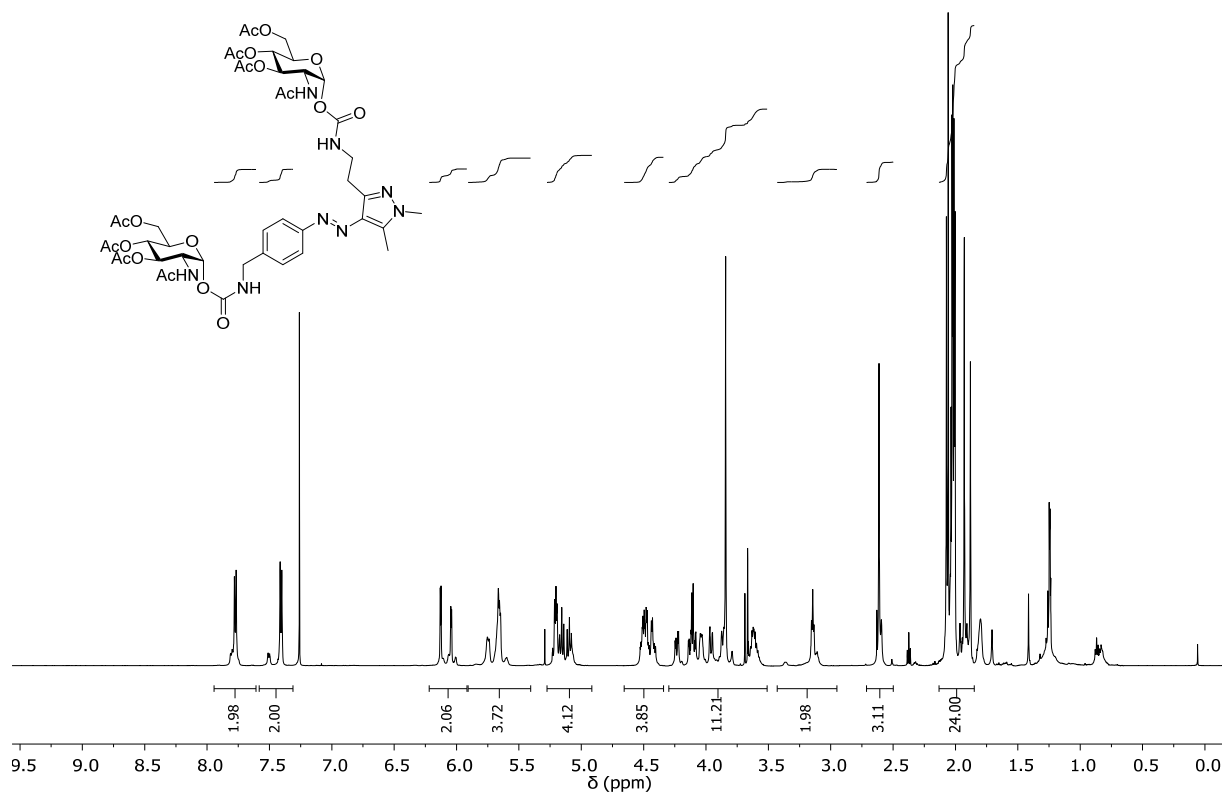
^1H NMR of **E-11** (CD_3OD , 600 MHz, 300 K).



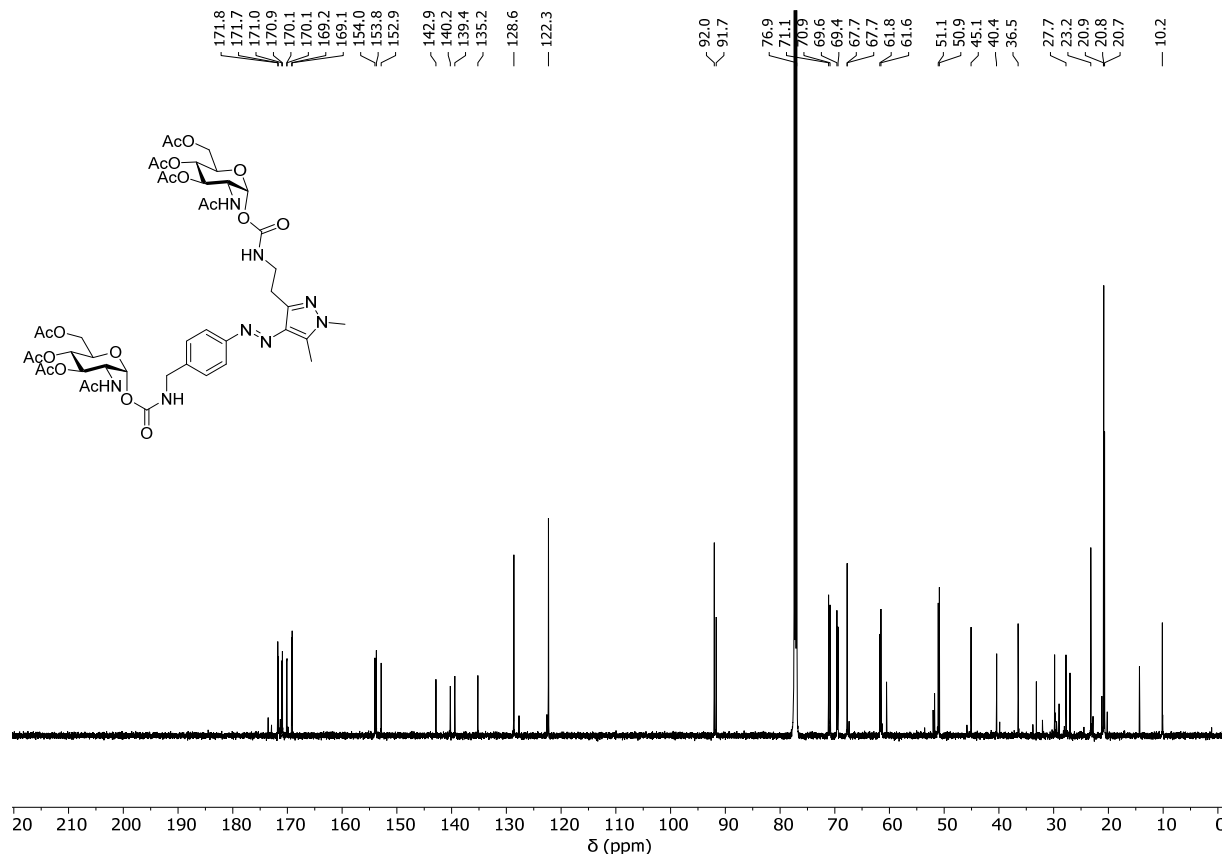
^{13}C NMR of **E-11** (CD_3OD , 151 MHz, 300 K).



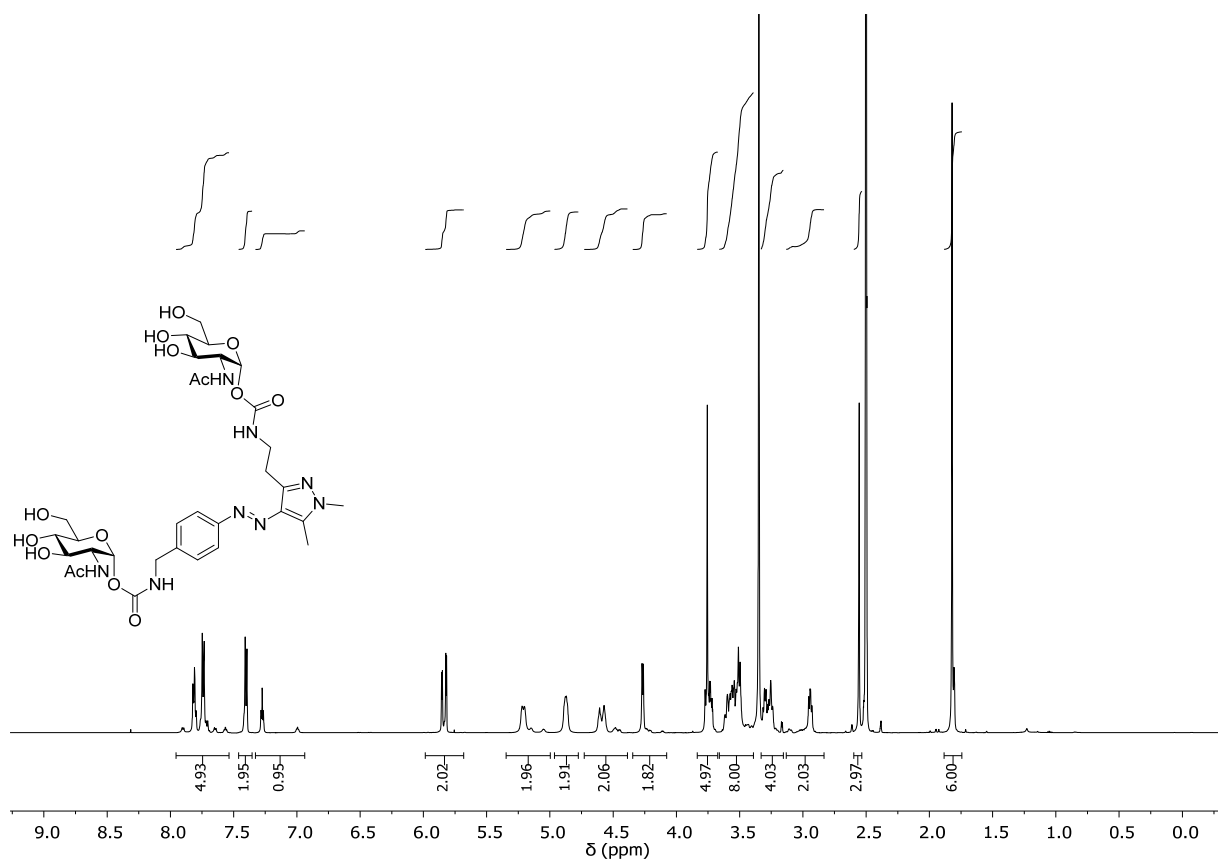
Section of HMBC NMR of **E-11** (CD_3OD , 600 MHz, 300 K).



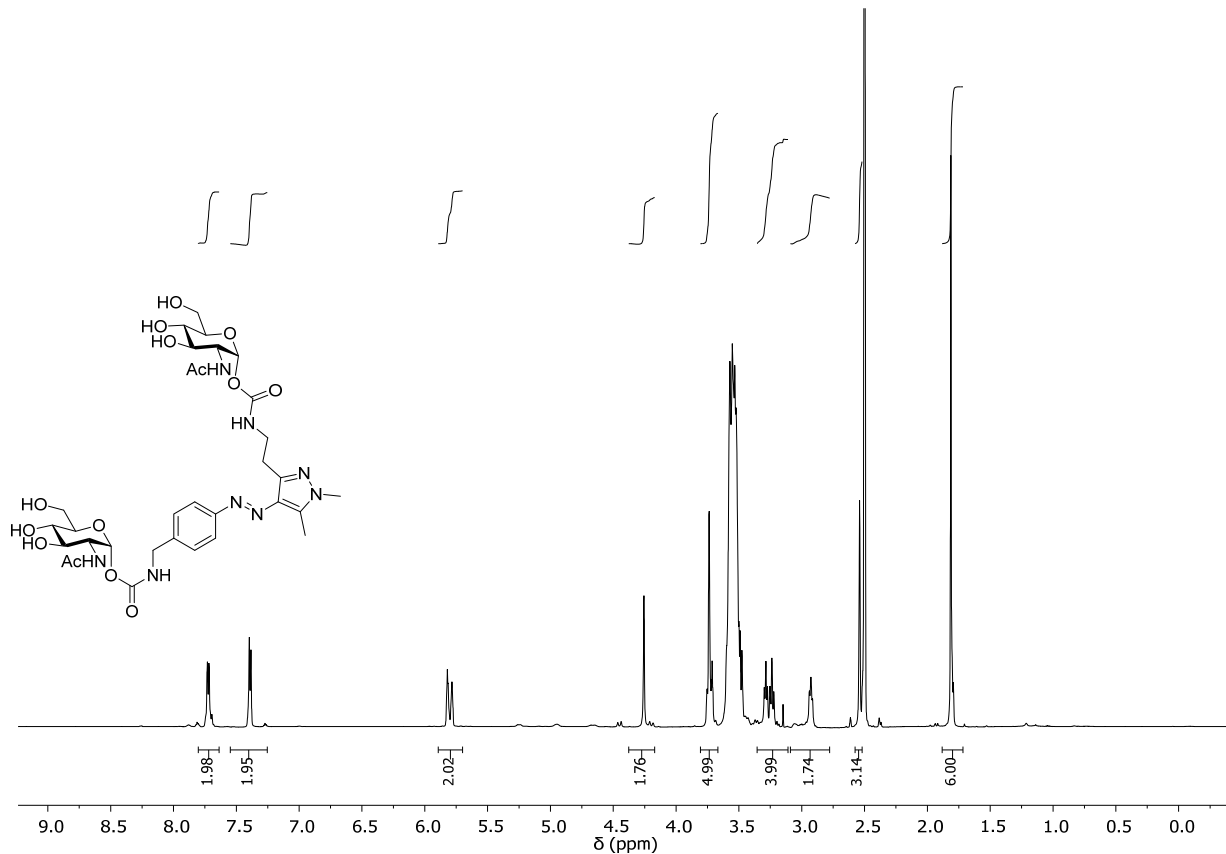
¹H NMR of HPLC-purified **E-13** (CDCl_3 , 600 MHz, 300 K). Several sets of signals are visible due to *E/Z* isomerization of the two carbamate groups.

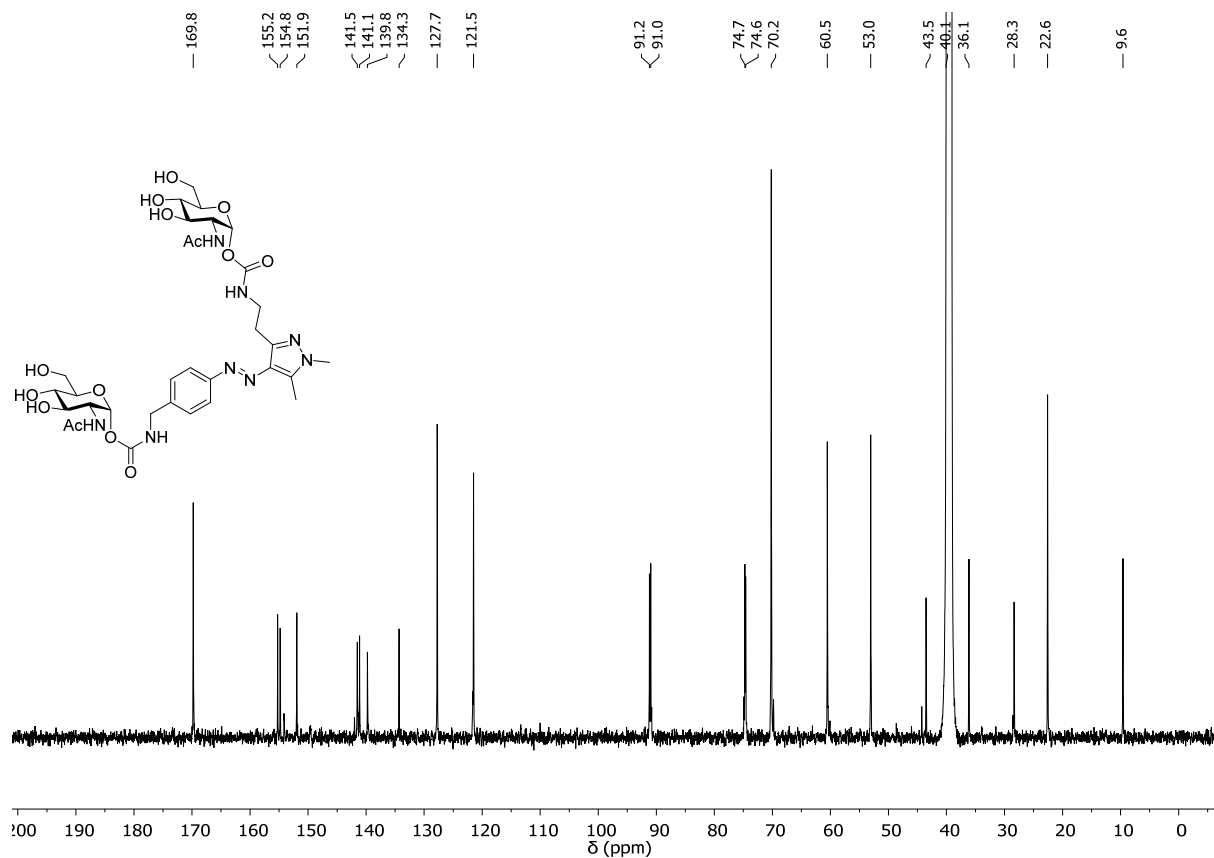


¹³C NMR of **E-13** (CDCl_3 , 151 MHz, 300 K)



¹H NMR of ligand **E-3** ($[D_6]DMSO$, 600 MHz, 300 K). Several sets of signals are visible due to *E/Z* isomerization of the two carbamate groups.





^{13}C NMR of ligand **E-3** ($[\text{D}_6]\text{DMSO}$, 151 MHz, 300 K).

8. References

- [1] C. E. Weston, R. D. Richardson, P. R. Haycock, A. J. P. White, M. J. Fuchter, *J. Am. Chem. Soc.* **2014**, *136*, 11878-11881.
- [2] S. R. Logan, *J. Chem. Educ.* **1997**, *74*, 1303.
- [3] While the Laser pulse energy was measured directly for 532 nm irradiation, this was not possible for irradiation with 355 nm as the pulse energies needed were too small. For this reason, higher laser pulse energies and an attenuator plate with known attenuation factor were used.
- [4] T. Wiseman, S. Williston, J. F. Brandts, L.-N. Lin, *Anal. Biochem.* **1989**, *179*, 131-137.
- [5] MATHEMATICA, Version 11.2, **2017**, Wolfram Research, Inc.: Champaign, Ill.